

University of São Paulo

São Carlos School of engineering



Legged Robots

Professor: Thiago Boaventura

Student: Jhon Charaja

Laboratory 4

Impedance Control

São Carlos - Brasil
2021 - 2

1 Joint space impedance control

1.1 PD impedance controllers

The objective of these activities is analyze effects of impedance parameters (\mathbf{M}_{des} , \mathbf{K}_{des} , \mathbf{D}_{des}) on the relation between interaction torques ($\boldsymbol{\tau}_{\text{ext}}$) and joint configuration (\mathbf{q} , $\dot{\mathbf{q}}$, $\ddot{\mathbf{q}}$). For this purpose, a simulation environment is developed that contains the UR5 robot and allows external torques to be applied. The simulation starts with initial joint configuration $\mathbf{q}_0 = \begin{bmatrix} 0.0 & -1.0 & 1.0 & 0.5 & 0.0 & 0.5 \end{bmatrix}$ rad and end-effector $\mathbf{p}_0 = \begin{bmatrix} 0.577 & 0.192 & 0.364 \end{bmatrix}$ m. Then, external torque $\boldsymbol{\tau}_{\text{ext}} = 20 \sin(2\pi t)$ is applied to each joint. The following subsections describe three desired dynamic behaviors: (i) stiffness, (ii) damping, (iii) stiffness and damping.

1.1.1 Only stiffness

The movements of ur5 robot is controlled with a proportional impedance control method at joint level. Thus, control law can be computed as

$$\boldsymbol{\tau} = \mathbf{K}_{\text{des}} \mathbf{e}, \quad (1)$$

where $\mathbf{e} = \mathbf{q}_{\text{des}} - \mathbf{q}$ is joint position error, and \mathbf{K}_{des} is desired stiffness.

Figure 1-3 show relation between external force ($\boldsymbol{\tau}_{\text{ext}}$) and joint configuration (\mathbf{q} , $\dot{\mathbf{q}}$, $\ddot{\mathbf{q}}$) using control law (1) with $\mathbf{K}_{\text{des}} = 500 \mathbf{I}_{6 \times 6} \frac{\text{N.m}}{\text{rad}}$. In these figures, the joints present different dynamic behaviors despite having the same control law. This is because the robot configuration generates different inertial and gravitational effects on each joint. In this context, the first three joints (q_1, q_2, q_3) are most affected by the weight of ur5 robot. For this reason, the last three joints (q_4, q_5, q_6) have similar graphs and maintain the dynamic relationship with the external force $\boldsymbol{\tau}_{\text{ext}}$; while the first three (q_1, q_2, q_3) have different graphs because the control law does not compensate for inertial and gravitational effects. Finally, the dynamic relationship of the last joint (q_6) is a line in position, circle in velocity and line with negative slope in acceleration. This can be analyzed in more detail with graphs of joint configuration (\mathbf{q} , $\dot{\mathbf{q}}$, $\ddot{\mathbf{q}}$) and external torque ($\boldsymbol{\tau}_{\text{ext}}$) versus time.

Figure 4-6 show joint configuration (\mathbf{q} , $\dot{\mathbf{q}}$, $\ddot{\mathbf{q}}$) and external torque ($\boldsymbol{\tau}_{\text{ext}}$) versus time. In these figures, joint configuration and external torque were normalized to obtain the same range of values¹. First, Figure 4 shows that q_6 is aligned in phase with $\boldsymbol{\tau}_{\text{ext}}$. Hence, the linear relationship between q_6 and $\boldsymbol{\tau}_{\text{ext}}$, described in Figure 1, can be justified. Second, Figure 5 shows that \dot{q}_6 leads $\boldsymbol{\tau}_{\text{ext}}$ by 90° . In this context,

¹The data was normalized with `normalize()` function of MATLAB.

τ_{ext} describes a $\sin(\cdot)$ function whereas q_6 describes a $\cos(\cdot)$ function. Hence, the circular relationship between \dot{q}_6 and τ_{ext} , described in Figure 2, can be justified. Finally, Figure 6 shows that τ_{ext} leads q_6 by 180° . In this context, τ_{ext} describes a $\sin(\cdot)$ function whereas \ddot{q}_6 describes a $-\sin(\cdot)$ function. Hence, the line with negative slope relationship between \ddot{q}_6 and τ_{ext} , described in Figure 3, can be justified.

The dynamic relation between τ_{ext} and q_6 could be analyzed using Laplace. It can be assumed, without generating large calculation errors, that the inertial and gravitational effects are close to 0 for the last joint (q_6). Thus, simplified dynamic equation of q_6 is $\ddot{q} = K_{\text{des}}q_{\text{des}} - K_{\text{des}}q + \tau_{\text{ext}}$. Then, representing in Laplace

$$q_6(s) = \frac{K_{\text{des}}q_{\text{des}}(s)}{s^2 + K_{\text{des}}} + \frac{1}{s^2 + K_{\text{des}}}\tau_{\text{ext}}(s),$$

where $\frac{K_{\text{des}}q_{\text{des}}}{s^2 + K_{\text{des}}}$ just add a constant value to the output signal and $G = \frac{1}{s^2 + k}$ is a filter that does not modify frequency. Hence, considering $\tau_{\text{ext}} = 20 \sin(2\pi t)$ as input, the output signal will be $q_6 \approx 0.5 + 0.04 \sin(2\pi t)$. Then, the linear relationship between q_6 and τ_{ext} could be justified. Second, time-derivative of q_6 could be approximated as $\dot{q}_6 \approx 0.251 \cos(2\pi t)$. Then, the circular relationship between \dot{q}_6 and τ_{ext} could be justified. Finally, time-derivative of \dot{q}_6 could be approximated as $\ddot{q}_6 \approx -1.58 \sin(2\pi t)$. Then, the line with negative slope relationship between \ddot{q}_6 and τ_{ext} could be justified.

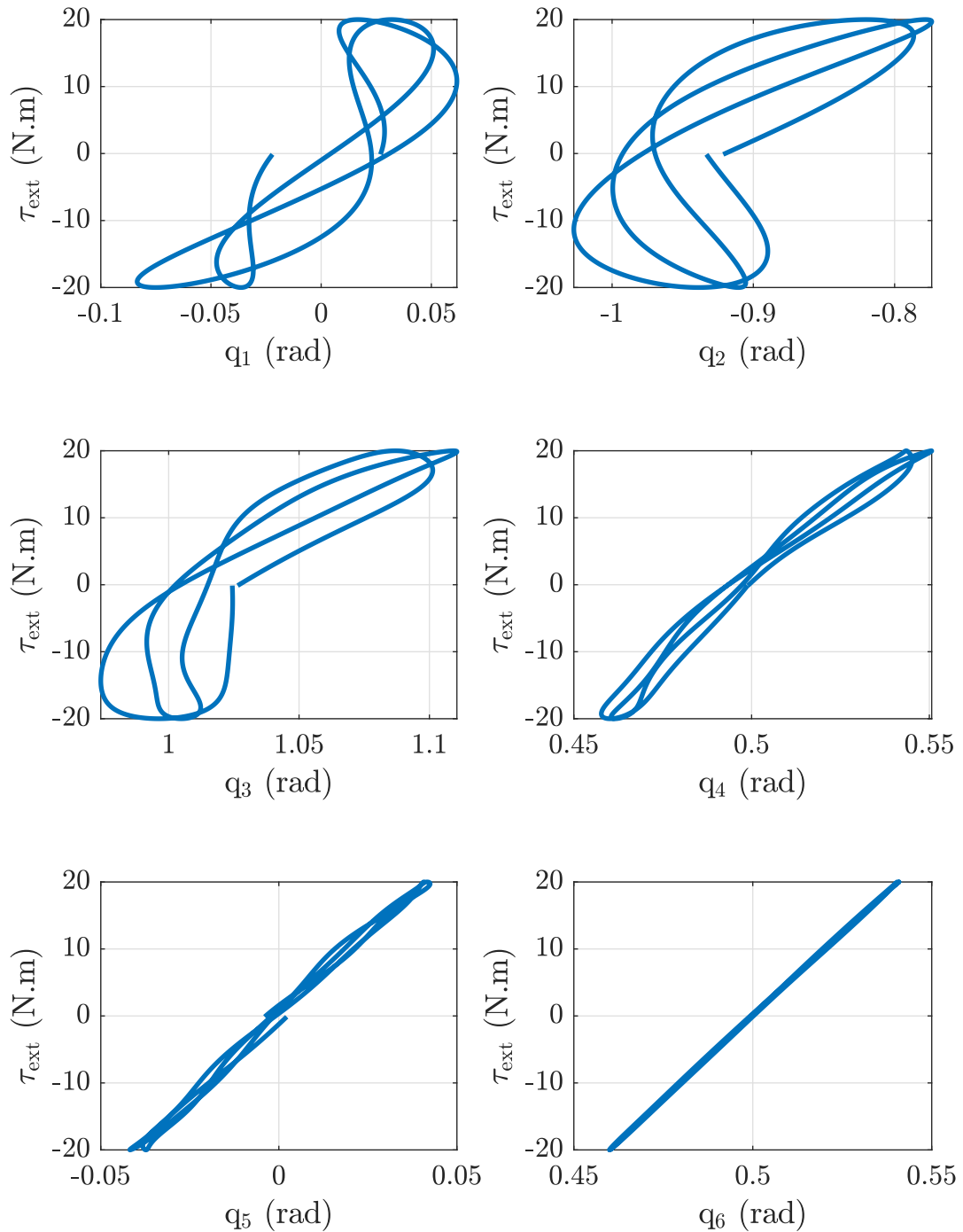


Figure 1: Dynamic relation between external torque (τ_{ext}) and joint positions (q) using proportional impedance control (1) with $\mathbf{K}_{\text{des}} = 500\mathbf{I}_{6 \times 6}$.

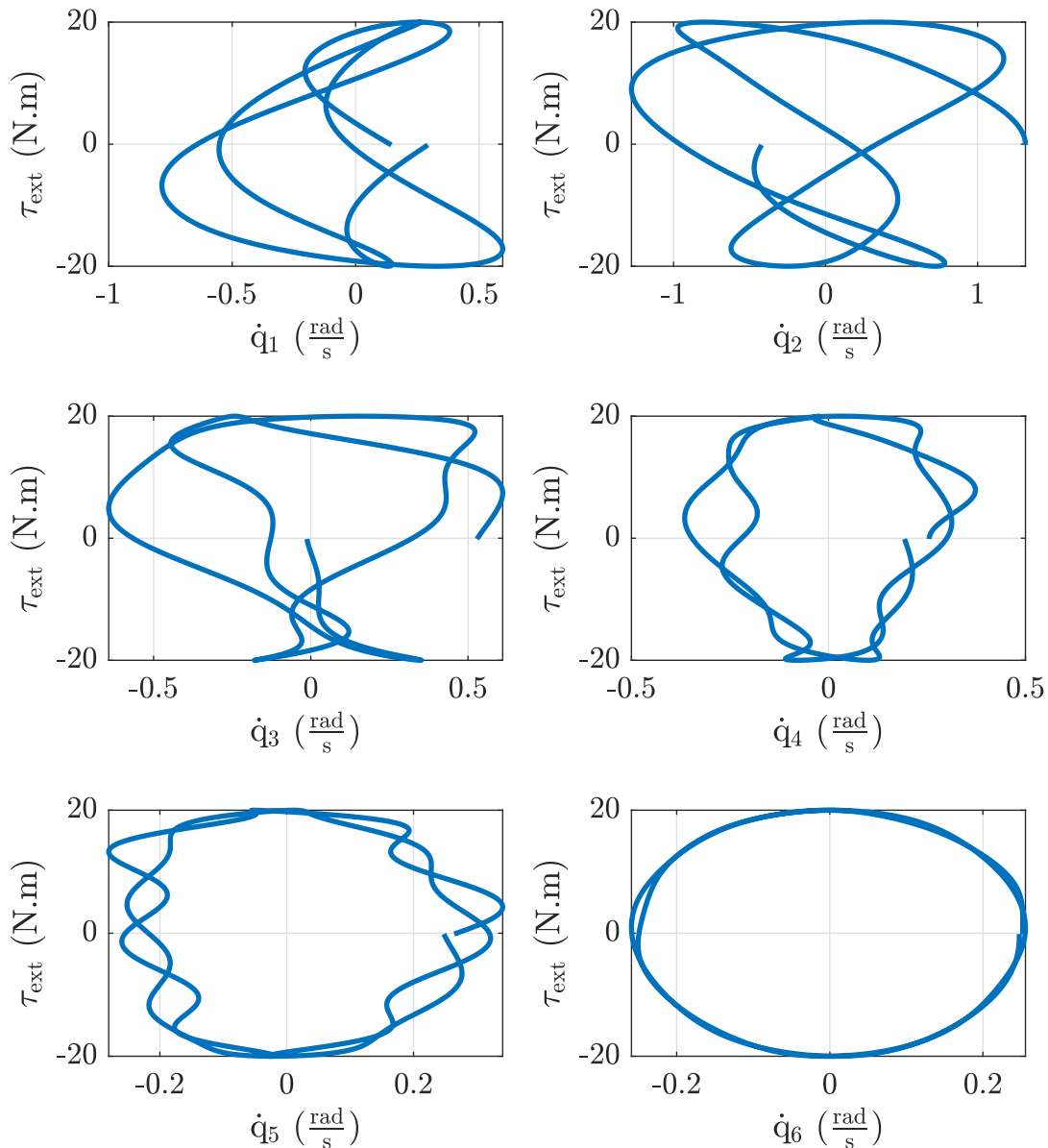


Figure 2: Dynamic relation between external torque (τ_{ext}) and joint velocities (\dot{q}) using proportional impedance control (1) with $K_{\text{des}} = 500I_{6 \times 6}$.

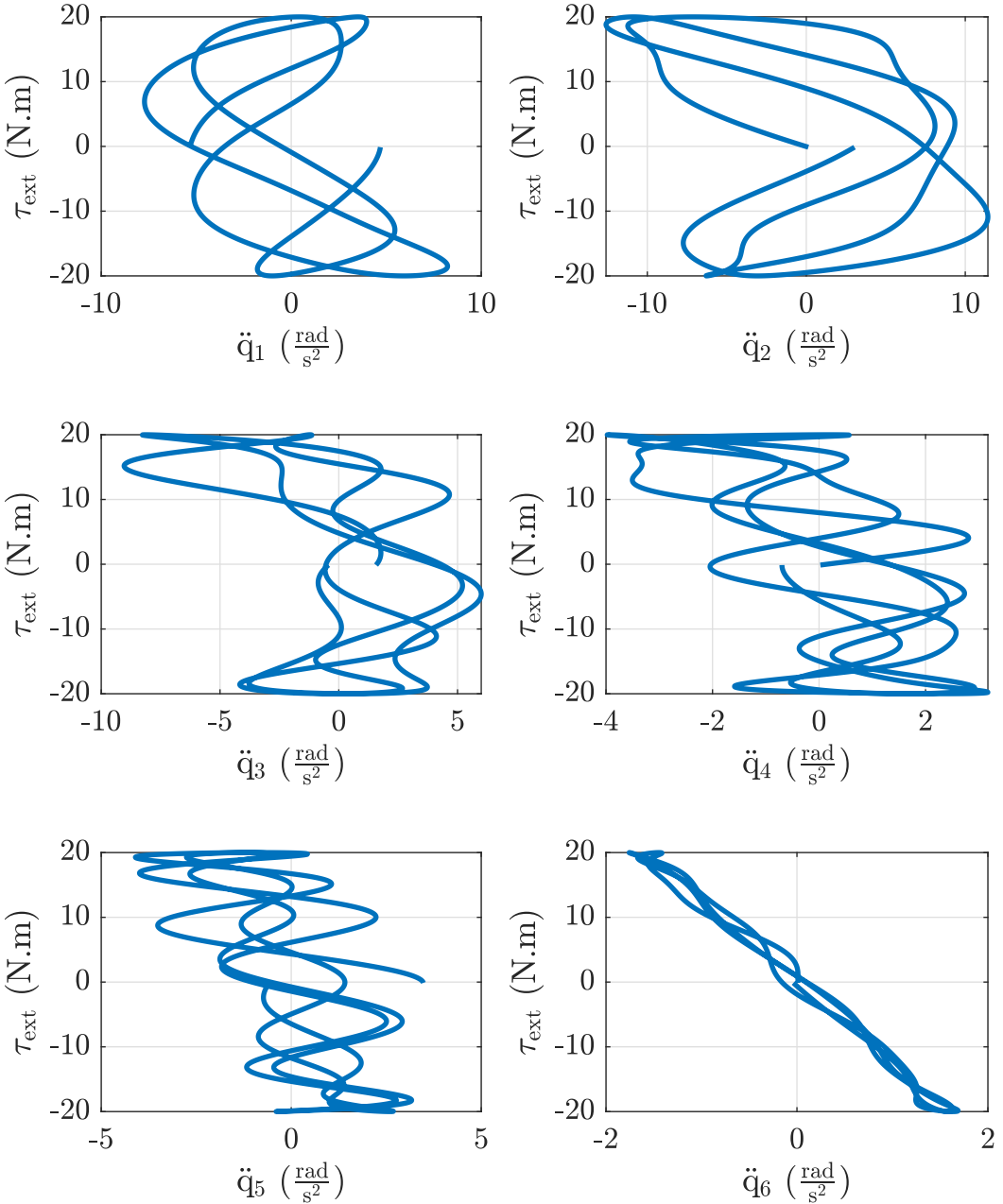


Figure 3: Dynamic relation between external torque (τ_{ext}) and joint accelerations (\ddot{q}) using proportional impedance control (1) with $\mathbf{K}_{\text{des}} = 500\mathbf{I}_{6 \times 6}$.

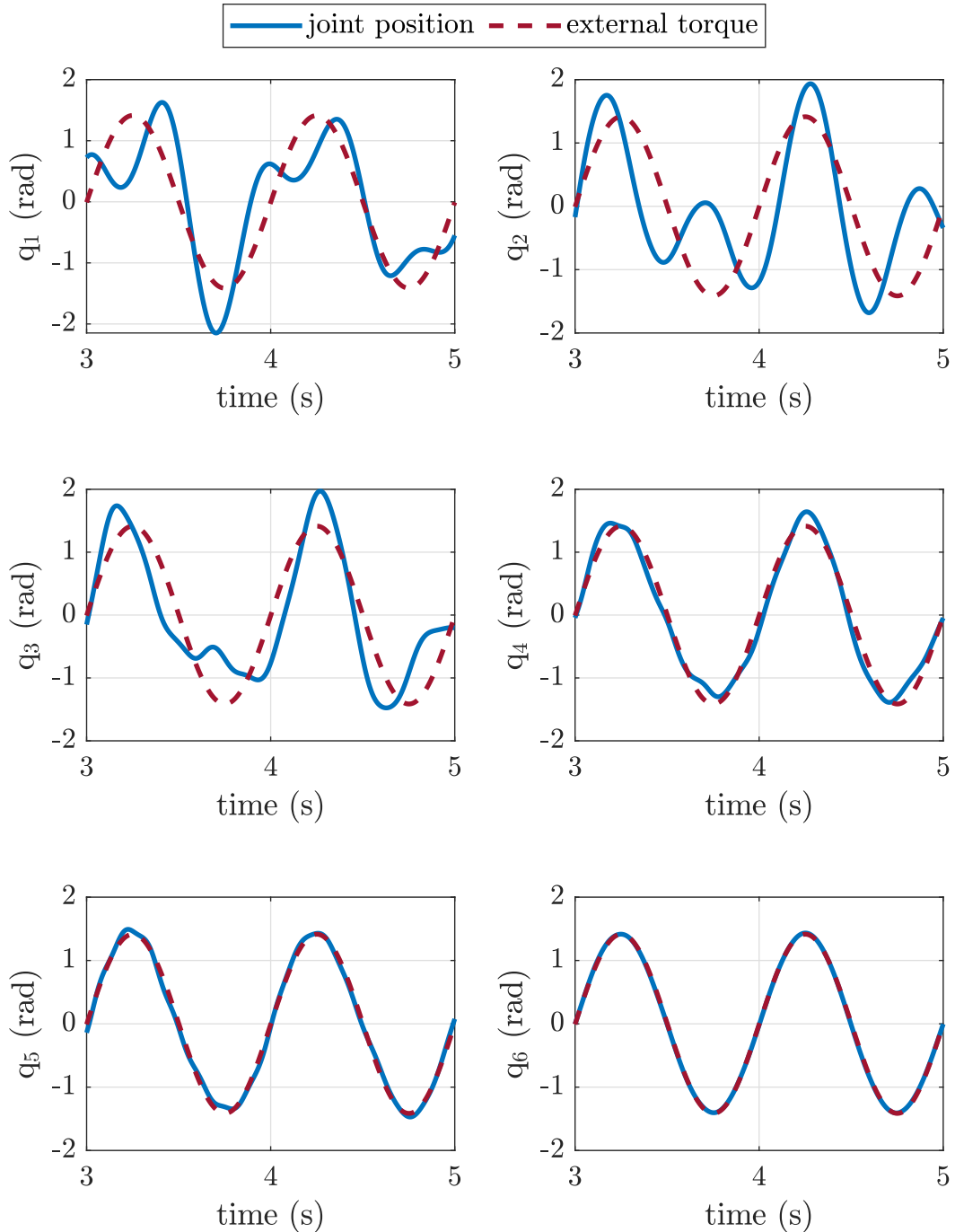


Figure 4: Normalized joint positions (\mathbf{q}) and external torque (τ_{ext}) with respect to time.

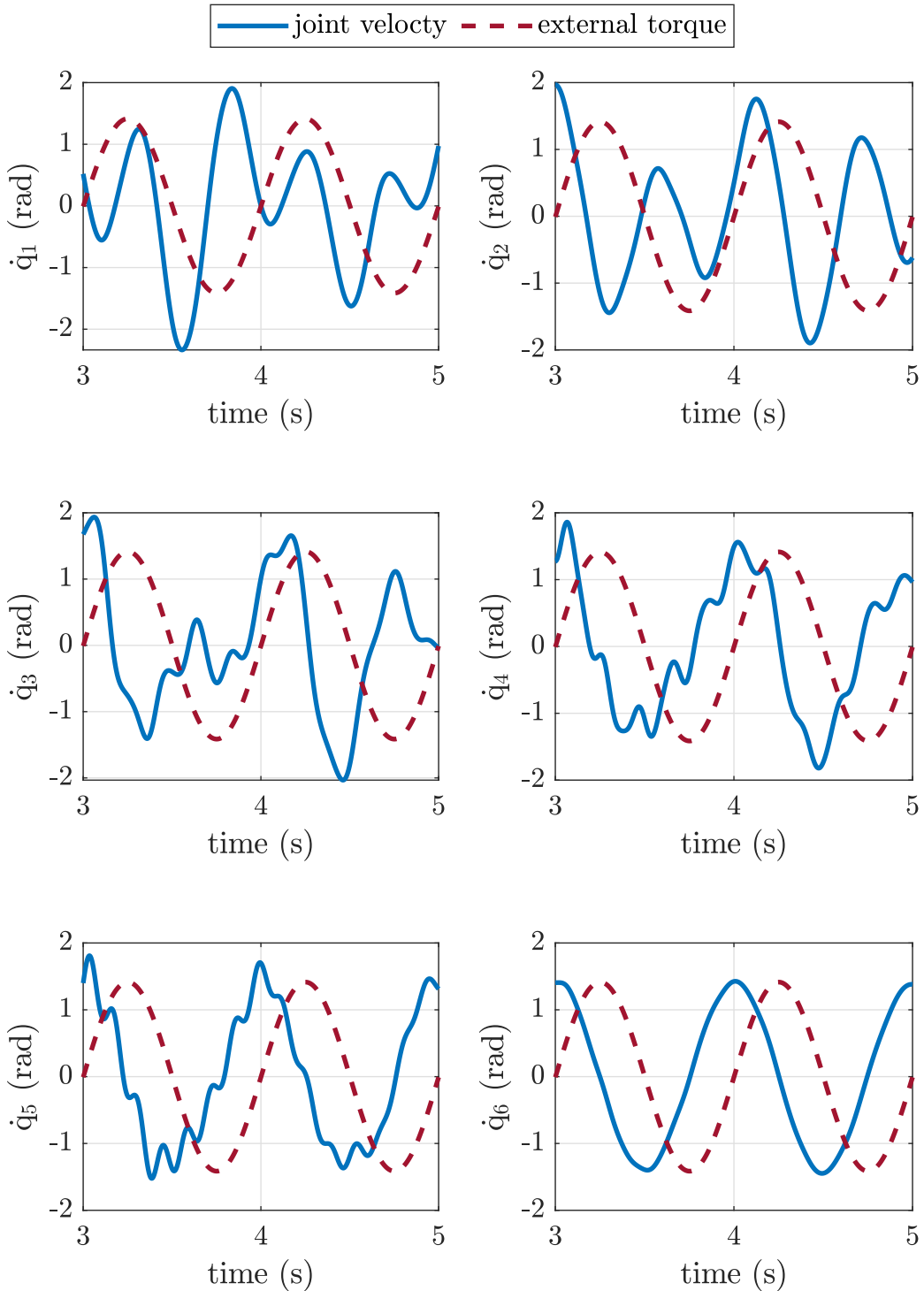


Figure 5: Normalized joint velocities (\dot{q}) and external torque (τ_{ext}) with respect to time.

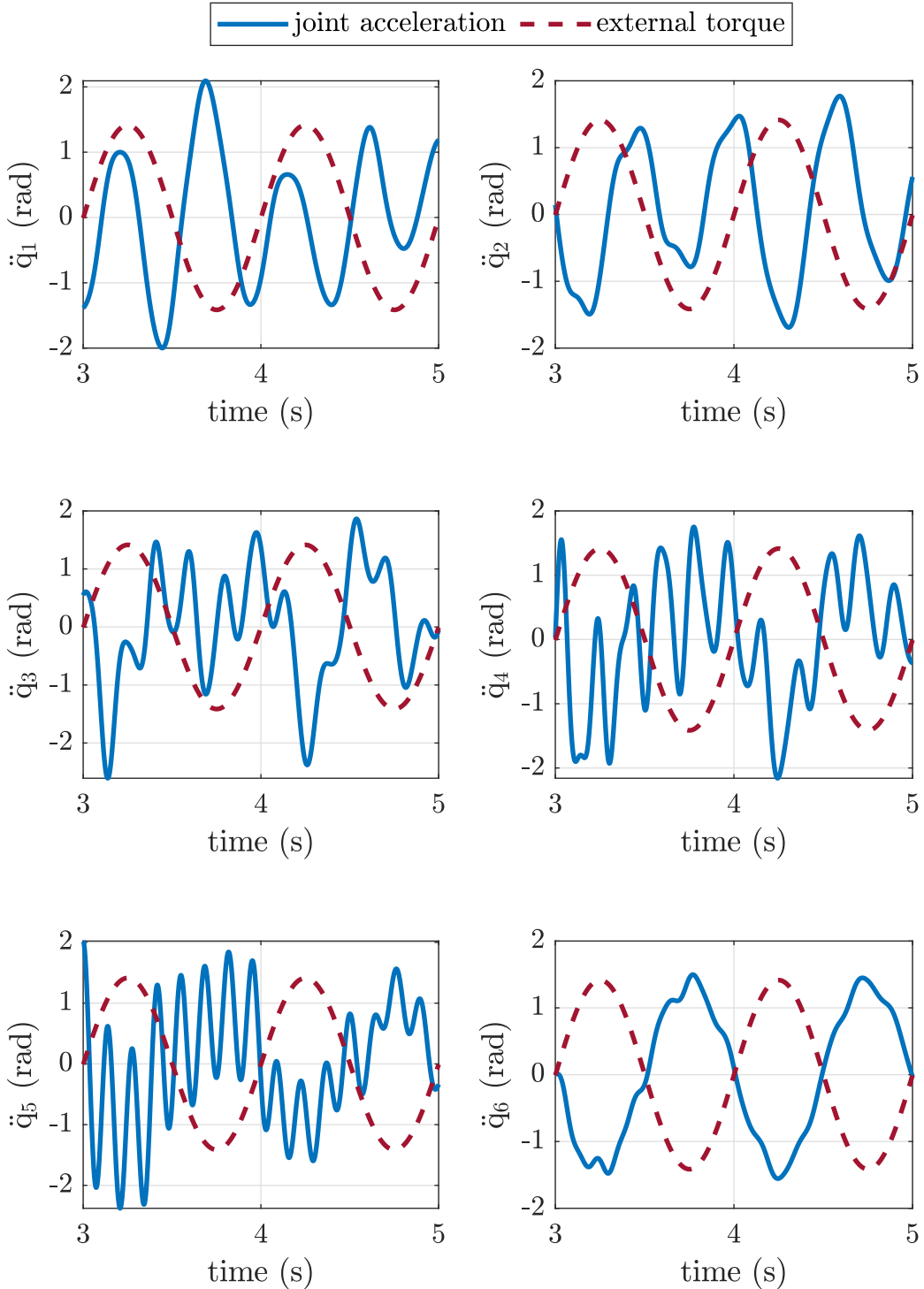


Figure 6: Normalized joint accelerations (\ddot{q}) and external torque (τ_{ext}) with respect to time.

1.1.2 Only damping

The movements of ur5 robot is controlled with a derivative impedance control method at joint level. Thus, control law can be computed as

$$\boldsymbol{\tau} = \mathbf{D}_{\text{des}} \dot{\mathbf{e}}, \quad (2)$$

where $\mathbf{e} = \mathbf{q}_{\text{des}} - \mathbf{q}$ is joint position error, and \mathbf{D}_{des} is desired damping.

Figure 7-9 show relation between external force ($\boldsymbol{\tau}_{\text{ext}}$) and joint configuration ($\mathbf{q}, \dot{\mathbf{q}}, \ddot{\mathbf{q}}$) using control law (2) with $\mathbf{D}_{\text{des}} = 10 \mathbf{I}_{6 \times 6} \frac{\text{N.m.s}}{\text{rad}}$. In these figures, the joints present different dynamic behaviors despite having the same control law. This is because the robot configuration generates different inertial and gravitational effects on each joint. In this context, the first three joints (q_1, q_2, q_3) are most affected by the weight of ur5 robot. For this reason, the last three joints (q_4, q_5, q_6) have similar graphs and maintain the dynamic relationship with the external force $\boldsymbol{\tau}_{\text{ext}}$; while the first three (q_1, q_2, q_3) have different graphs because the control law does not compensate for inertial and gravitational effects. Finally, the dynamic relationship of the last joint (q_6) is a circle in position, line in velocity and circle in acceleration. This can be analyzed in more detail with graphs of joint configuration and external torque versus time.

Figure 10-12 show joint configuration ($\mathbf{q}, \dot{\mathbf{q}}, \ddot{\mathbf{q}}$) and external torque ($\boldsymbol{\tau}_{\text{ext}}$) versus time. In these figures, joint configuration and external torque were normalized to obtain the same range of values². First, Figure 10 shows that $\boldsymbol{\tau}_{\text{ext}}$ leads q_6 by 90° . In this context, $\boldsymbol{\tau}_{\text{ext}}$ describes a $\sin(\cdot)$ function whereas q_6 describes a $-\cos(\cdot)$ function. Hence, the circular relationship between q_6 and $\boldsymbol{\tau}_{\text{ext}}$, described in Figure 7, can be justified. Second, Figure 11 shows that \dot{q}_6 is aligned in phase with $\boldsymbol{\tau}_{\text{ext}}$. Hence, the line relationship between \dot{q}_6 and $\boldsymbol{\tau}_{\text{ext}}$, described in Figure 8, can be justified. Finally, Figure 12 shows that \ddot{q}_6 leads $\boldsymbol{\tau}_{\text{ext}}$ by 90° . In this context, $\boldsymbol{\tau}_{\text{ext}}$ describes a $\sin(\cdot)$ function whereas \ddot{q}_6 describes a $\cos(\cdot)$ function. Hence, the circular relationship between \ddot{q}_6 and $\boldsymbol{\tau}_{\text{ext}}$, described in Figure 9, can be justified.

The relation between $\boldsymbol{\tau}_{\text{ext}}$ and q_6 could be analyzed using Laplace. It can be assumed, without generating large calculation errors, that the inertial and gravitational effects are close to 0 for the last joint (q_6). Thus, simplified dynamic equation of q_6 is $\ddot{q} = D_{\text{des}} \dot{q}_{\text{des}} - D_{\text{des}} \dot{q} + \boldsymbol{\tau}_{\text{ext}}$. Then, representing in Laplace

$$\dot{q}_6(s) = \frac{D_{\text{des}} \dot{q}_{\text{des}}(s)}{s + D_{\text{des}}} + \frac{1}{s + D_{\text{des}}} \boldsymbol{\tau}_{\text{ext}}(s),$$

²The data was normalized with `normalize()` function of MATLAB.

where $\frac{D_{\text{des}}\dot{q}_{\text{des}}(s)}{s+D_{\text{des}}}$ just add a constant value to the output signal and $G = \frac{1}{s+D_{\text{des}}}$ is a filter that does not modify frequency of input signal. Hence, considering $\tau_{\text{ext}} = 20 \sin(2\pi t)$ as input, the output signal will be $\dot{q}_6 \approx 1.70 \sin(2\pi t)$. Then, the linear relationship between \dot{q}_6 and τ_{ext} could be justified. Second, time-derivative of \dot{q}_6 could be approximated as $\ddot{q}_6 \approx 10.6 \cos(2\pi t)$. Then, circular relationship between \ddot{q}_6 and τ_{ext} could be justified.

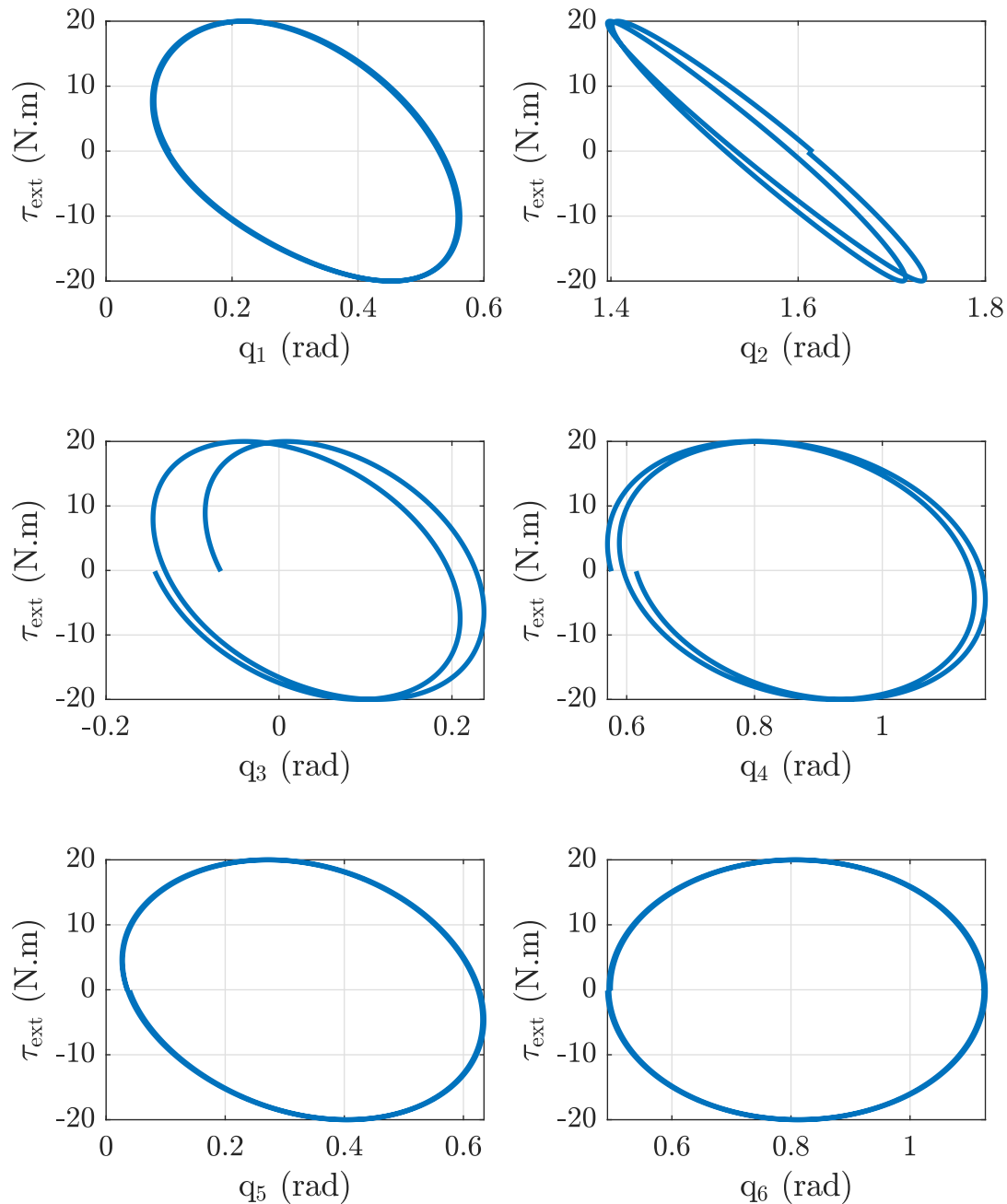


Figure 7: Dynamic relation between external torque (τ_{ext}) and joint positions (q) using proportional impedance control (2) with $\mathbf{D}_{\text{des}} = 10\mathbf{I}_{6 \times 6} \frac{\text{N.m.s}}{\text{rad}}$.

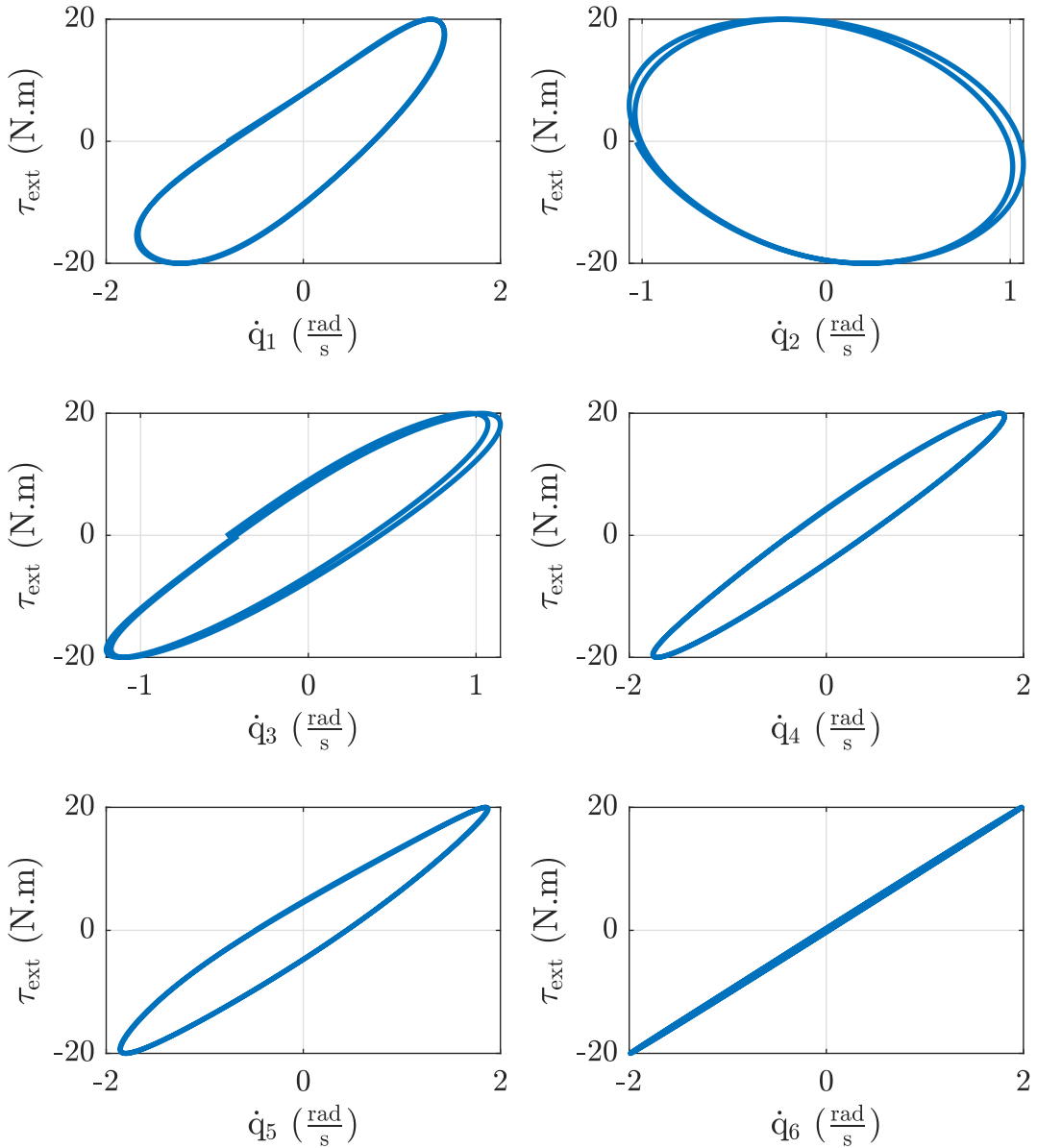


Figure 8: Dynamic relation between external torque (τ_{ext}) and joint velocities (\dot{q}) using proportional impedance control (2) with $\mathbf{D}_{\text{des}} = 10\mathbf{I}_{6 \times 6} \frac{\text{N.m.s}}{\text{rad}}$.

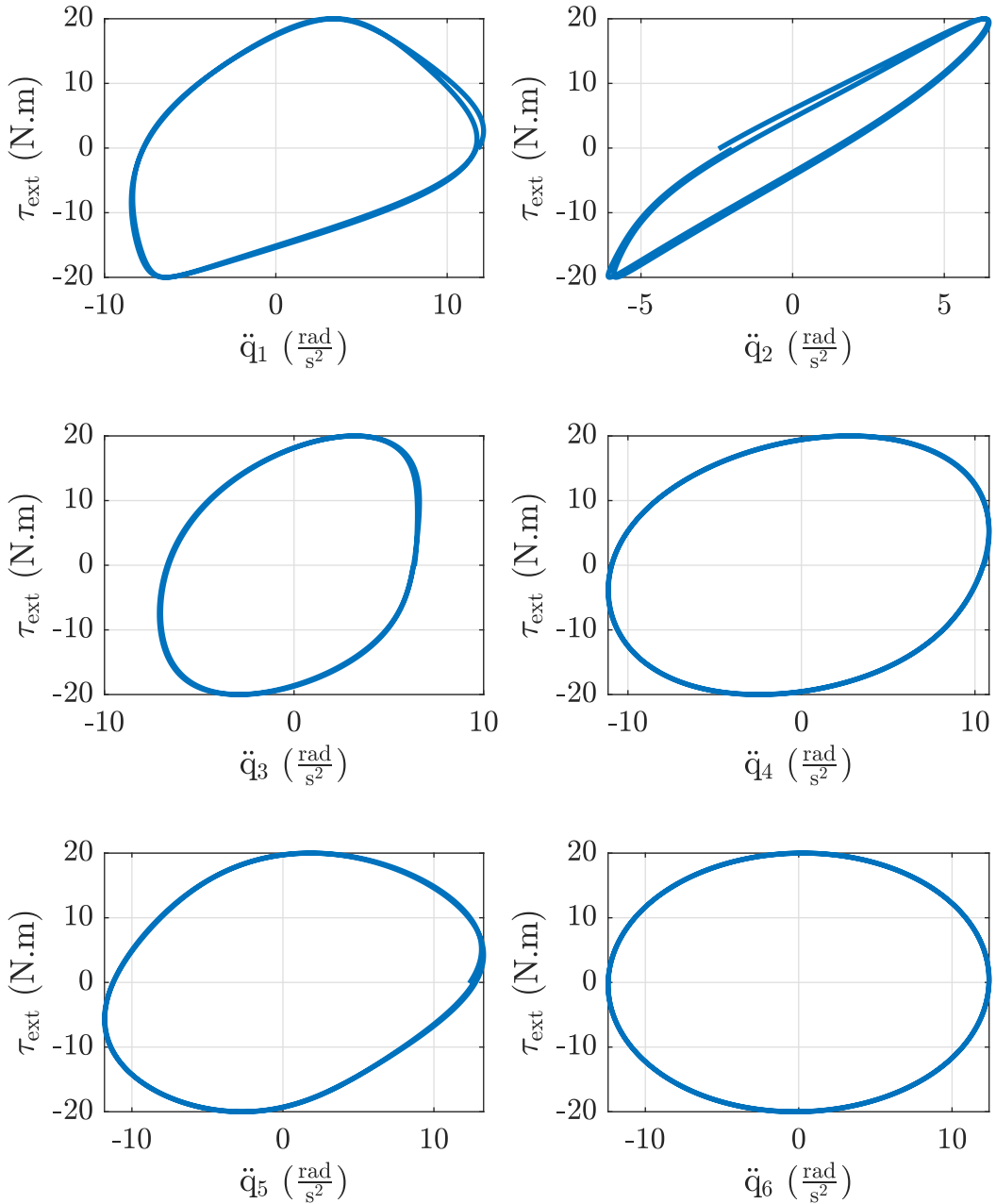


Figure 9: Dynamic relation between external torque (τ_{ext}) and joint accelerations (\ddot{q}) using proportional impedance control (2) with $D_{\text{des}} = 10I_{6 \times 6} \frac{\text{N.m.s}}{\text{rad}}$.

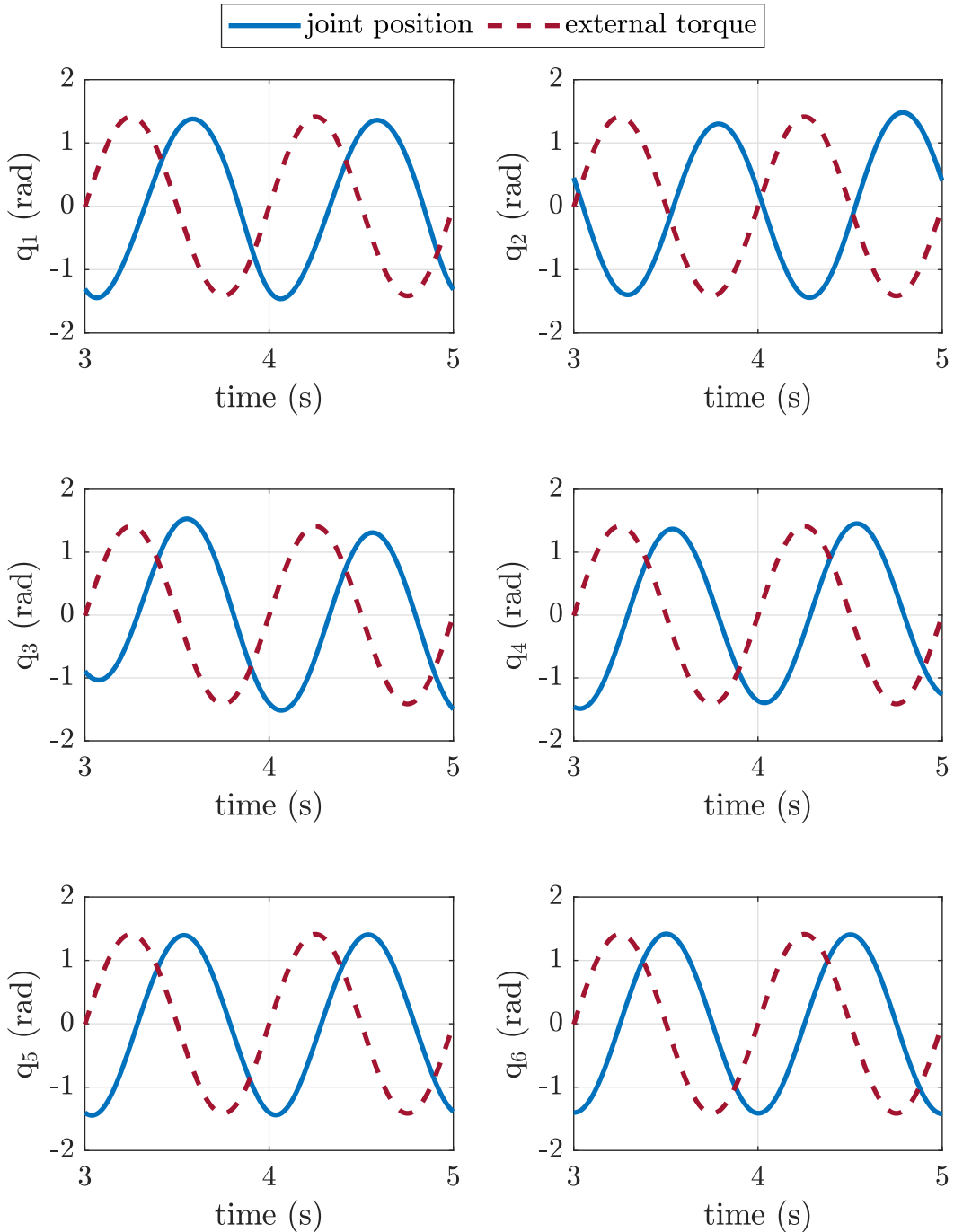


Figure 10: Normalized joint positions (\mathbf{q}) and external torque ($\boldsymbol{\tau}_{ext}$) with respect to time.

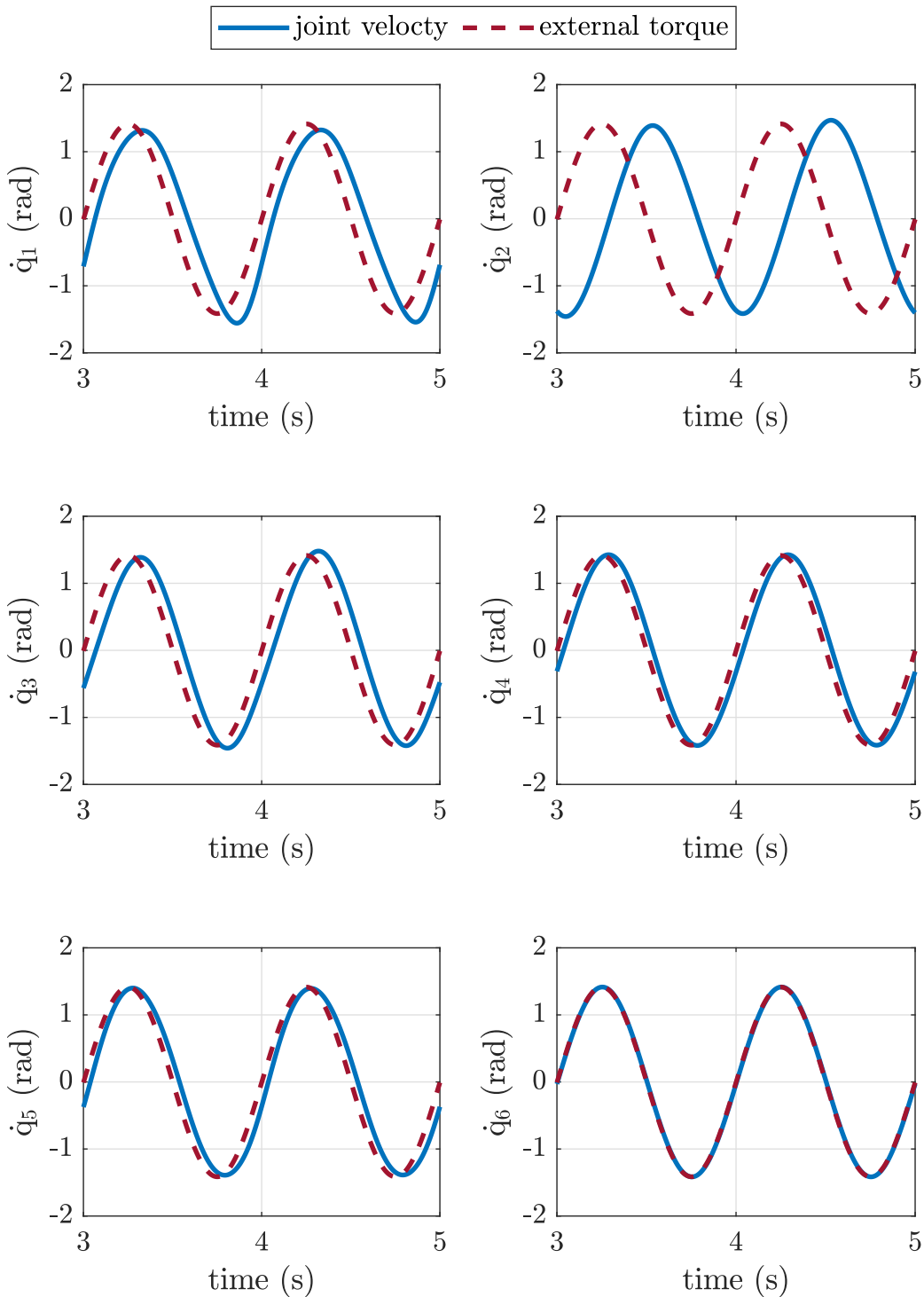


Figure 11: Normalized joint velocities (\dot{q}) and external torque (τ_{ext}) with respect to time.

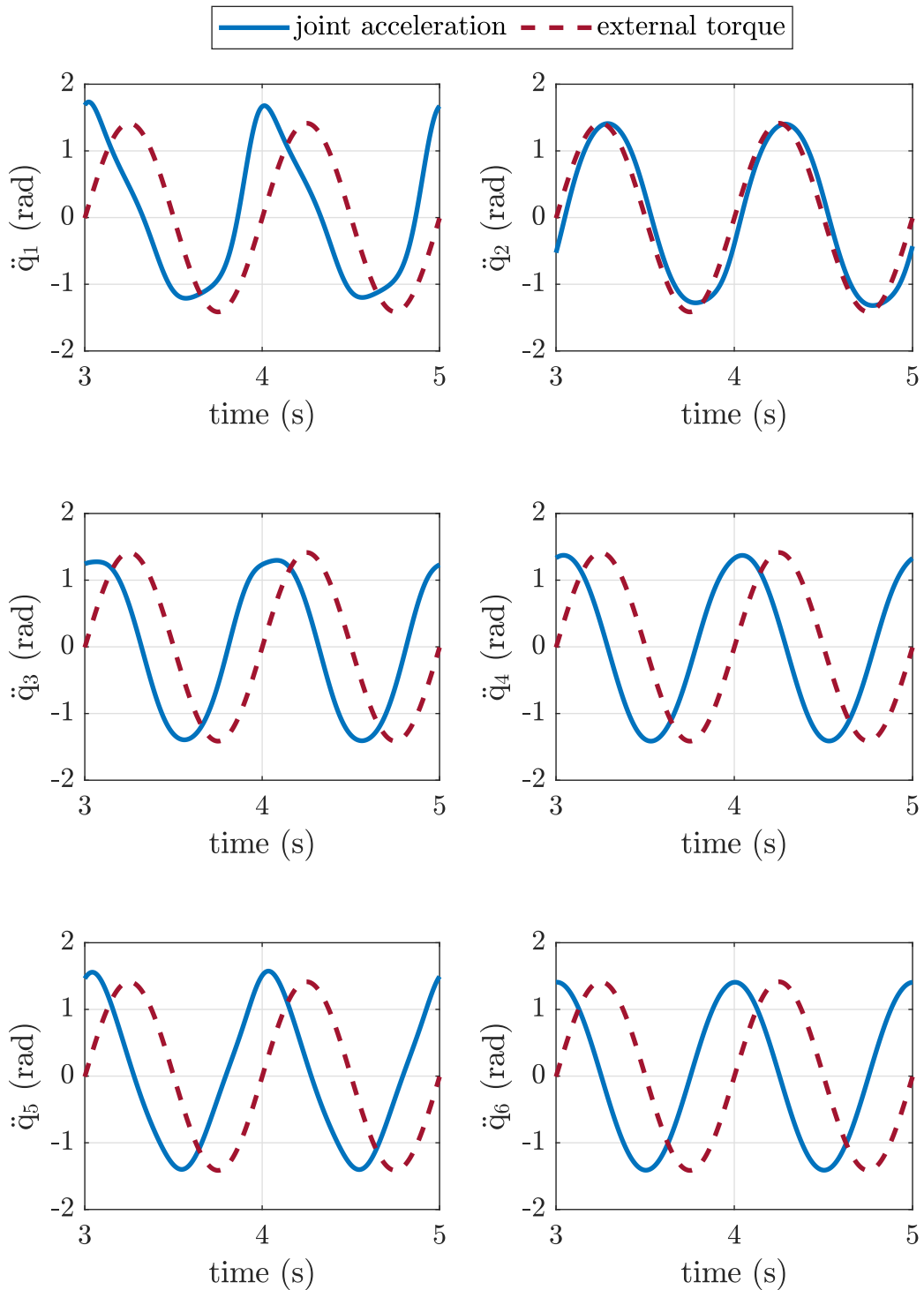


Figure 12: Normalized joint accelerations (\ddot{q}) and external torque (τ_{ext}) with respect to time.

1.1.3 Stiffness and Damping ($K = 500 \frac{\text{Nm}}{\text{rad}}$, $D = 10 \frac{\text{Nms}}{\text{rad}}$)

The movements of ur5 robot is controlled with a proportional-derivative impedance control method at joint level. Thus, control law can be computed as

$$\boldsymbol{\tau} = \mathbf{K}_{\text{des}} \mathbf{e} + \mathbf{D}_{\text{des}} \dot{\mathbf{e}}, \quad (3)$$

where $\mathbf{e} = \mathbf{q}_{\text{des}} - \mathbf{q}$ is joint position error, and $\mathbf{K}_{\text{des}}, \mathbf{D}_{\text{des}}$ are desired stiffness and damping, respectively.

Figure 13-15 show relation between external force ($\boldsymbol{\tau}_{\text{ext}}$) and joint configuration ($\mathbf{q}, \dot{\mathbf{q}}, \ddot{\mathbf{q}}$) using control law (3) with $\mathbf{K}_{\text{des}} = 500 \mathbf{I}_{6 \times 6} \frac{\text{N.m}}{\text{rad}}$ and $\mathbf{D}_{\text{des}} = 10 \mathbf{I}_{6 \times 6} \frac{\text{N.m.s}}{\text{rad}}$. In these figures, the joints present different dynamic behaviors despite having the same control law. This is because the robot configuration generates different inertial and gravitational effects on each joint. In this context, the first three joints (q_1, q_2, q_3) are most affected by the weight of ur5 robot. For this reason, the last three joints (q_4, q_5, q_6) have similar graphs and maintain the dynamic relationship with the external force $\boldsymbol{\tau}_{\text{ext}}$; while the first three (q_1, q_2, q_3) have different graphs because the control law does not compensate for inertial and gravitational effects. Finally, the dynamic behavior of the last joint (q_6) is a combination of Figure 1 and 7. Hence, stiffness set maximum joint position displacement ($\Delta q = 0.04 \text{ rad}$) whereas damping set maximum/minimum velocity ($\dot{q} = \pm 2 \frac{\text{rad}}{\text{s}}$). Consequently, impedance control with stiffness and damping parameters set a working space (position and velocity) and dynamic behavior when robot interact with external torques.

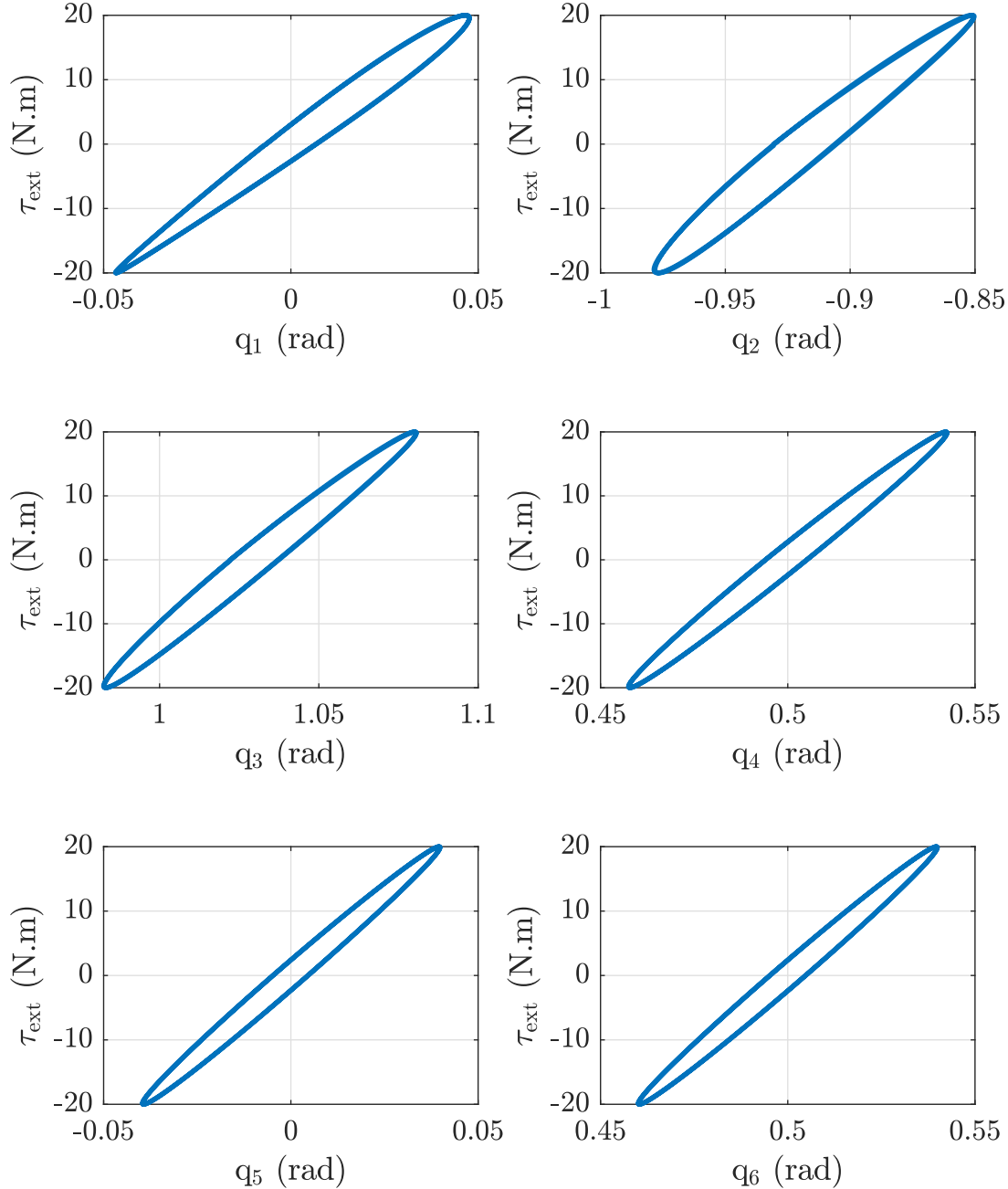


Figure 13: Dynamic relation between external torque (τ_{ext}) and joint positions (q) using proportional-derivative impedance control (3) with $\mathbf{K}_{\text{des}} = 500\mathbf{I}_{6 \times 6} \frac{\text{N.m}}{\text{rad}}$, $\mathbf{D}_{\text{des}} = 10\mathbf{I}_{6 \times 6}$ and $\frac{\text{N.m.s}}{\text{rad}}$.

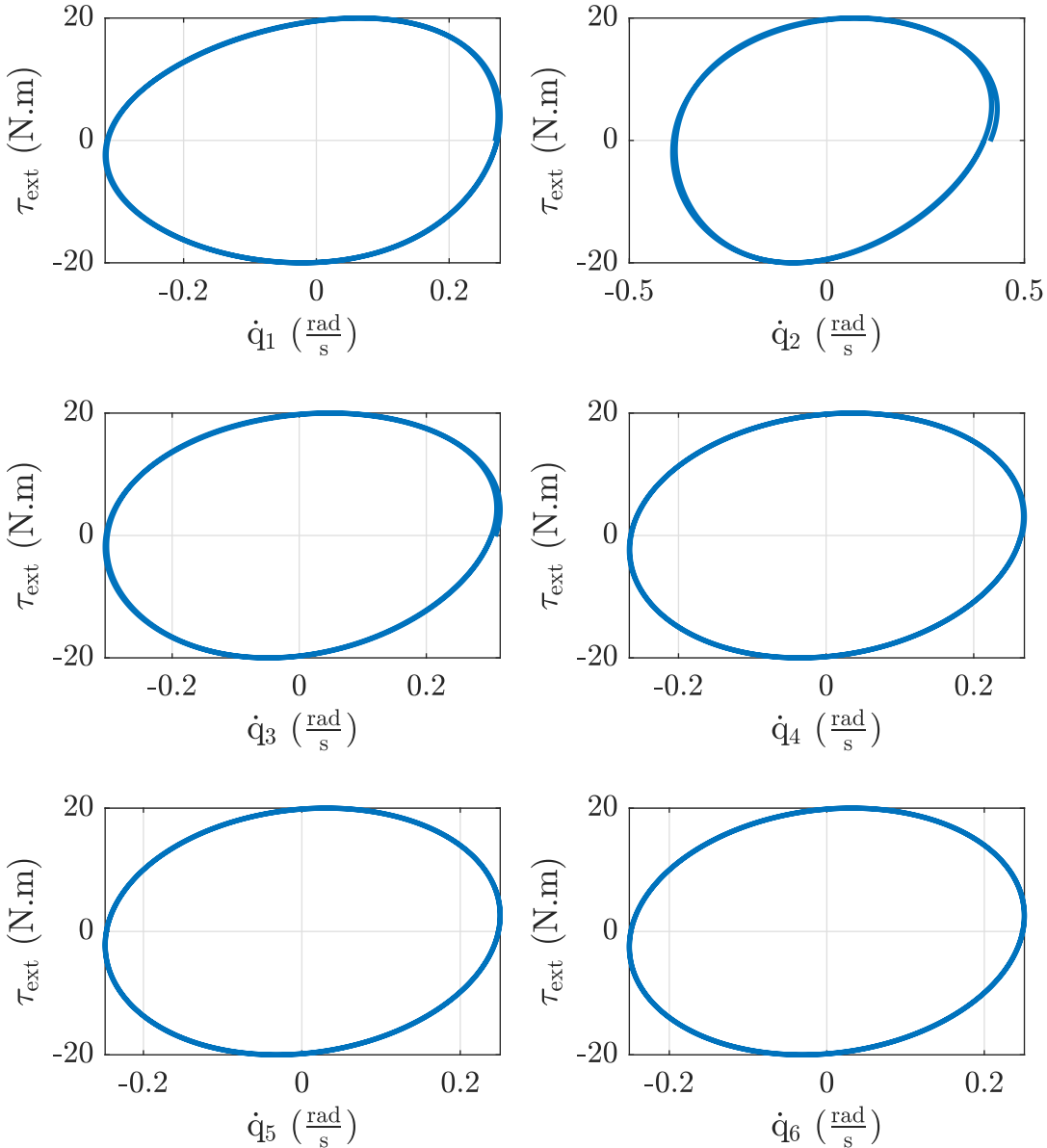


Figure 14: Dynamic relation between external torque (τ_{ext}) and joint velocities (\dot{q}) using proportional-derivative impedance control (3) with $\mathbf{K}_{\text{des}} = 500 \mathbf{I}_{6 \times 6} \frac{\text{N.m}}{\text{rad}}$, $\mathbf{D}_{\text{des}} = 10 \mathbf{I}_{6 \times 6}$ and $\frac{\text{N.m.s}}{\text{rad}}$.

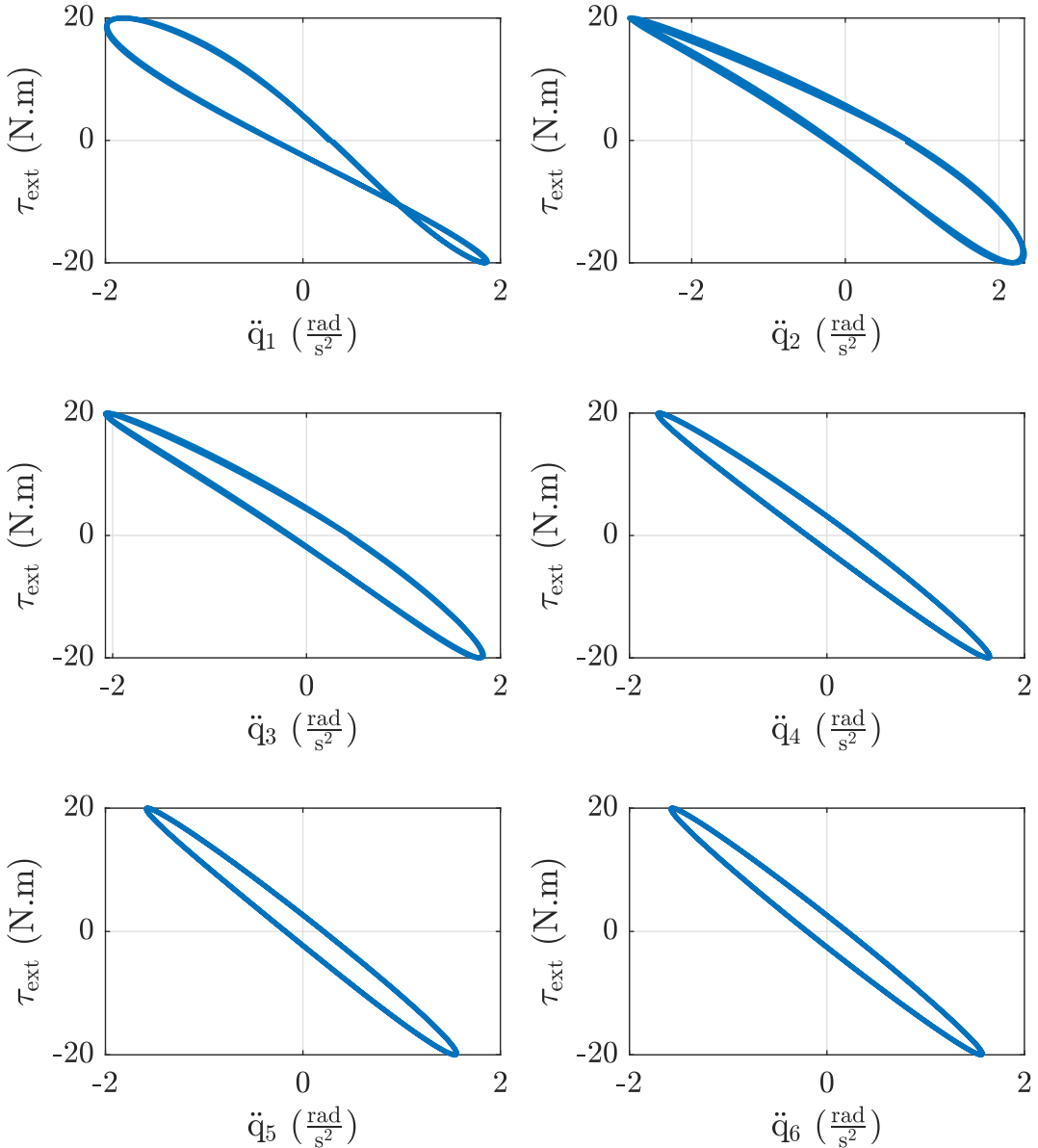


Figure 15: Dynamic relation between external torque (τ_{ext}) and joint accelerations (\ddot{q}) using proportional-derivative impedance control (3) with $\mathbf{K}_{\text{des}} = 500 \mathbf{I}_{6 \times 6} \frac{\text{N.m}}{\text{rad}}$, $\mathbf{D}_{\text{des}} = 10 \mathbf{I}_{6 \times 6}$ and $\frac{\text{N.m.s}}{\text{rad}}$.

1.2 Gravity and Coriolis compensation

The objective of this activity is analyze effects of gravity and Coriolis terms on the relation between interaction torques (τ_{ext}) and joint configuration ($\mathbf{q}, \dot{\mathbf{q}}, \ddot{\mathbf{q}}$). For this purpose, a simulation environment is developed that contains the UR5 robot and allows external torques to be applied. The simulation starts with initial joint configuration $\mathbf{q}_0 = [0.0 \ -1.0 \ 1.0 \ 0.5 \ 0.0 \ 0.5]$ rad. Then, external torque $\tau_{\text{ext}} = 20 \sin(2\pi t)$ is applied to each joint. Finally, movements of ur5 robot is controlled with a proportional-derivative impedance control method with gravity compensation at joint level. Thus, control law can be computed as

$$\boldsymbol{\tau} = \mathbf{K}_{\text{des}} \mathbf{e} + \mathbf{D}_{\text{des}} \dot{\mathbf{e}} + \mathbf{b}, \quad (4)$$

where $\mathbf{e} = \mathbf{q}_{\text{des}} - \mathbf{q}$ is joint position error, $\mathbf{b} = \mathbf{C}(\mathbf{q}, \dot{\mathbf{q}}) + \mathbf{g}(\mathbf{q})$ is nonlinear effects vector, and $\mathbf{D}_{\text{des}}, \mathbf{K}_{\text{des}}$ are desired stiffness and damping matrix, respectively.

Figure 16-18 show relation between external force (τ_{ext}) and joint configuration ($\mathbf{q}, \dot{\mathbf{q}}, \ddot{\mathbf{q}}$) using control law (4) with $\mathbf{K}_{\text{des}} = 500 \mathbf{I}_{6 \times 6} \frac{\text{N.m}}{\text{rad}}$ and $\mathbf{D}_{\text{des}} = 10 \mathbf{I}_{6 \times 6} \frac{\text{N.m.s}}{\text{rad}}$. First, Figure 16 shows relation between external torque (τ_{ext}) and joint positions (\mathbf{q}). In this figure, impedance profiles are similar at end-tip unlike Figure 13. However, the profiles have different widths at middle. Second, Figure 17 shows relation between external torque (τ_{ext}) and joint velocities ($\dot{\mathbf{q}}$). In this figure, impedance profiles are similar but not symmetrical. Finally, Figure 18 shows relation between external torque (τ_{ext}) and joint accelerations ($\ddot{\mathbf{q}}$). In this figure, impedance profiles have different widths at middle and shapes at end-tip. The differences in impedance profiles (τ_{ext} vs $\mathbf{q}, \dot{\mathbf{q}}, \ddot{\mathbf{q}}$) are generated because the ur5 robot generates different inertia effects on each joint. Finally, impedance profiles can be improved by compensating for inertial effects at control law.

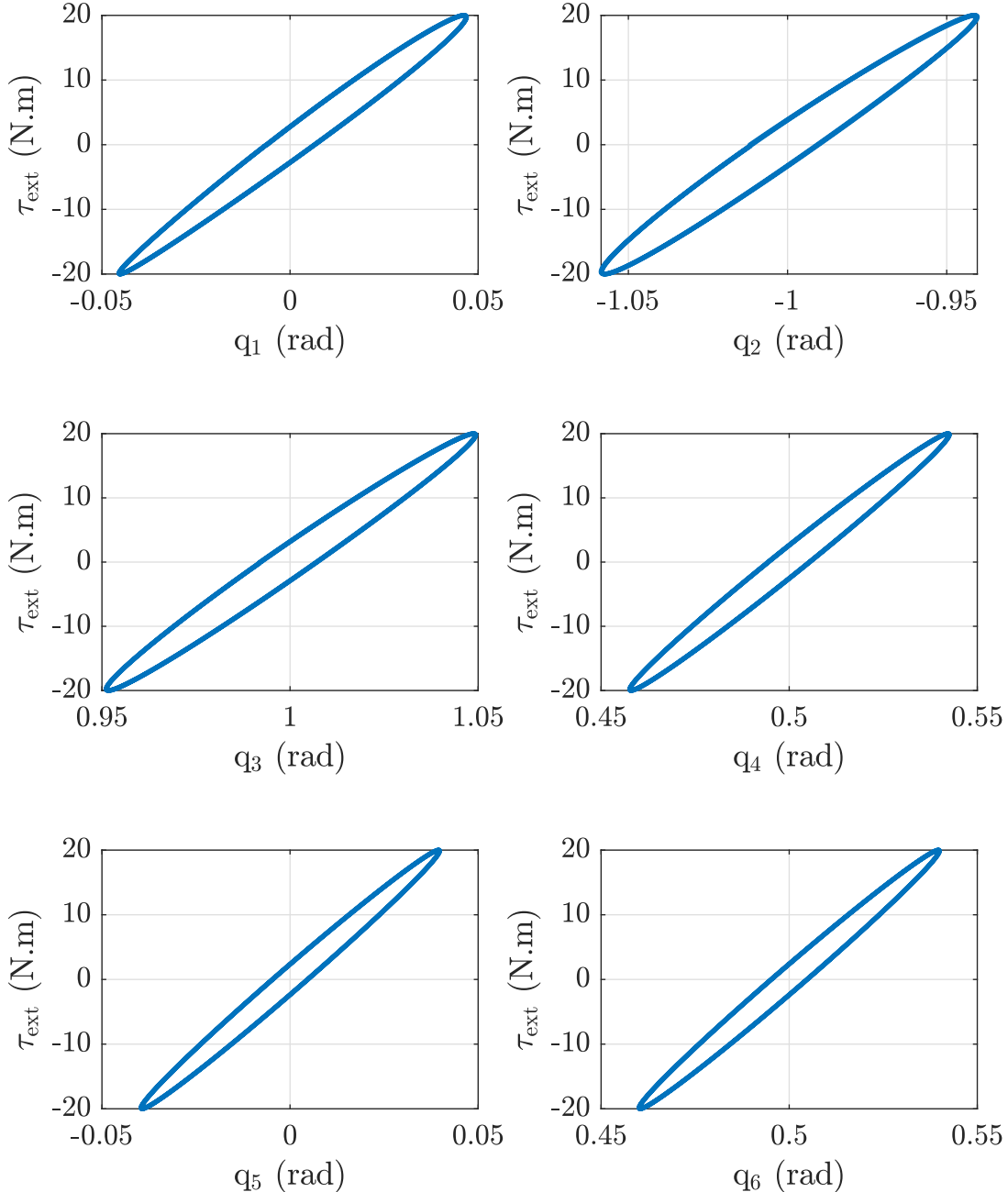


Figure 16: Dynamic relation between external torque (τ_{ext}) and joint positions (\mathbf{q}) using proportional-derivative impedance control with gravity compensation (4)
with $\mathbf{K}_{\text{des}} = 500 \mathbf{I}_{6 \times 6} \frac{\text{N.m}}{\text{rad}}$ $\mathbf{D}_{\text{des}} = 10 \mathbf{I}_{6 \times 6}$ and $\frac{\text{N.m.s}}{\text{rad}}$.

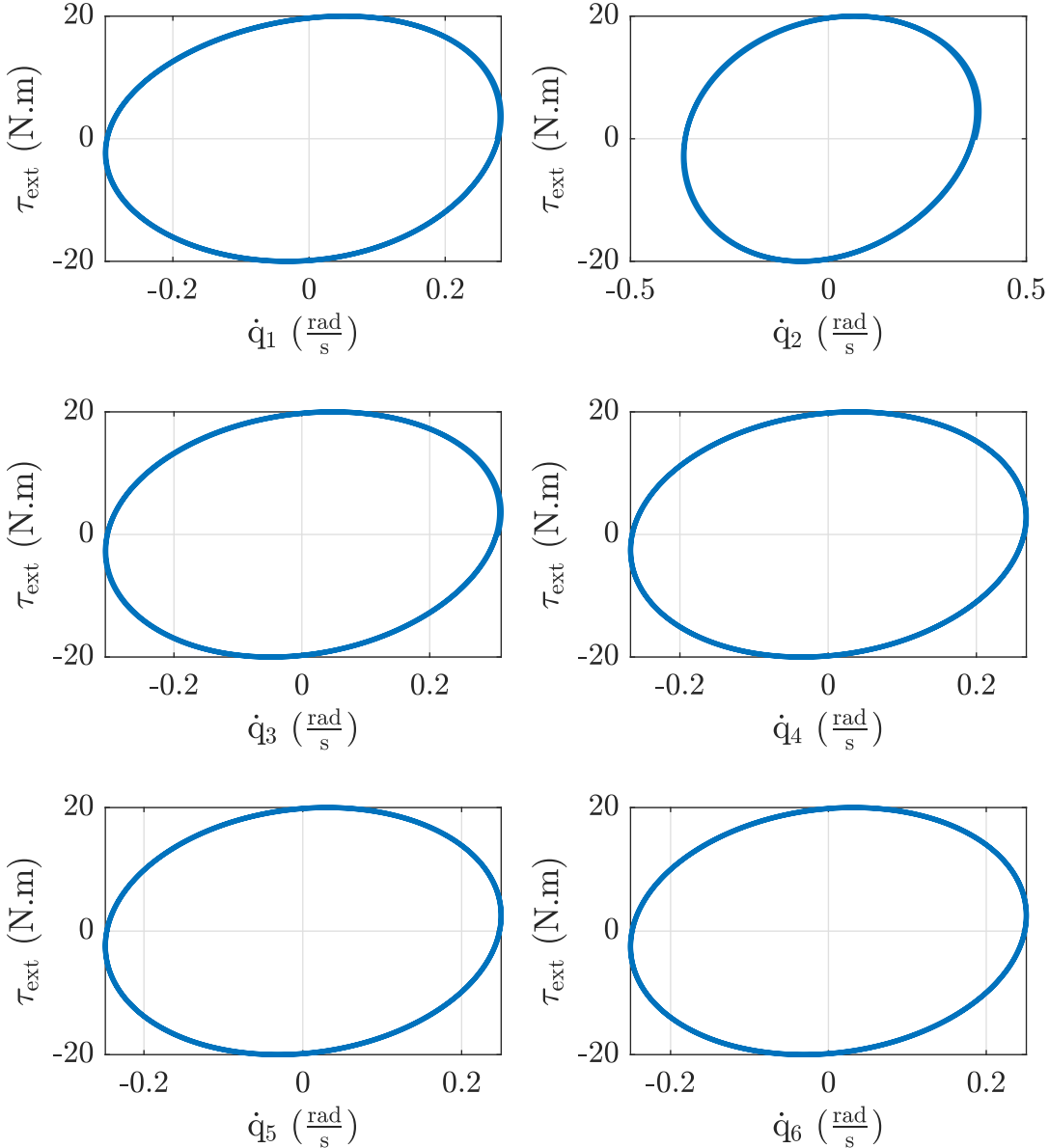


Figure 17: Dynamic relation between external torque (τ_{ext}) and joint velocities (\dot{q}) using proportional-derivative impedance control with gravity compensation (4)
with $\mathbf{K}_{\text{des}} = 500 \mathbf{I}_{6 \times 6} \frac{\text{N.m}}{\text{rad}}$ $\mathbf{D}_{\text{des}} = 10 \mathbf{I}_{6 \times 6}$ and $\frac{\text{N.m.s}}{\text{rad}}$.

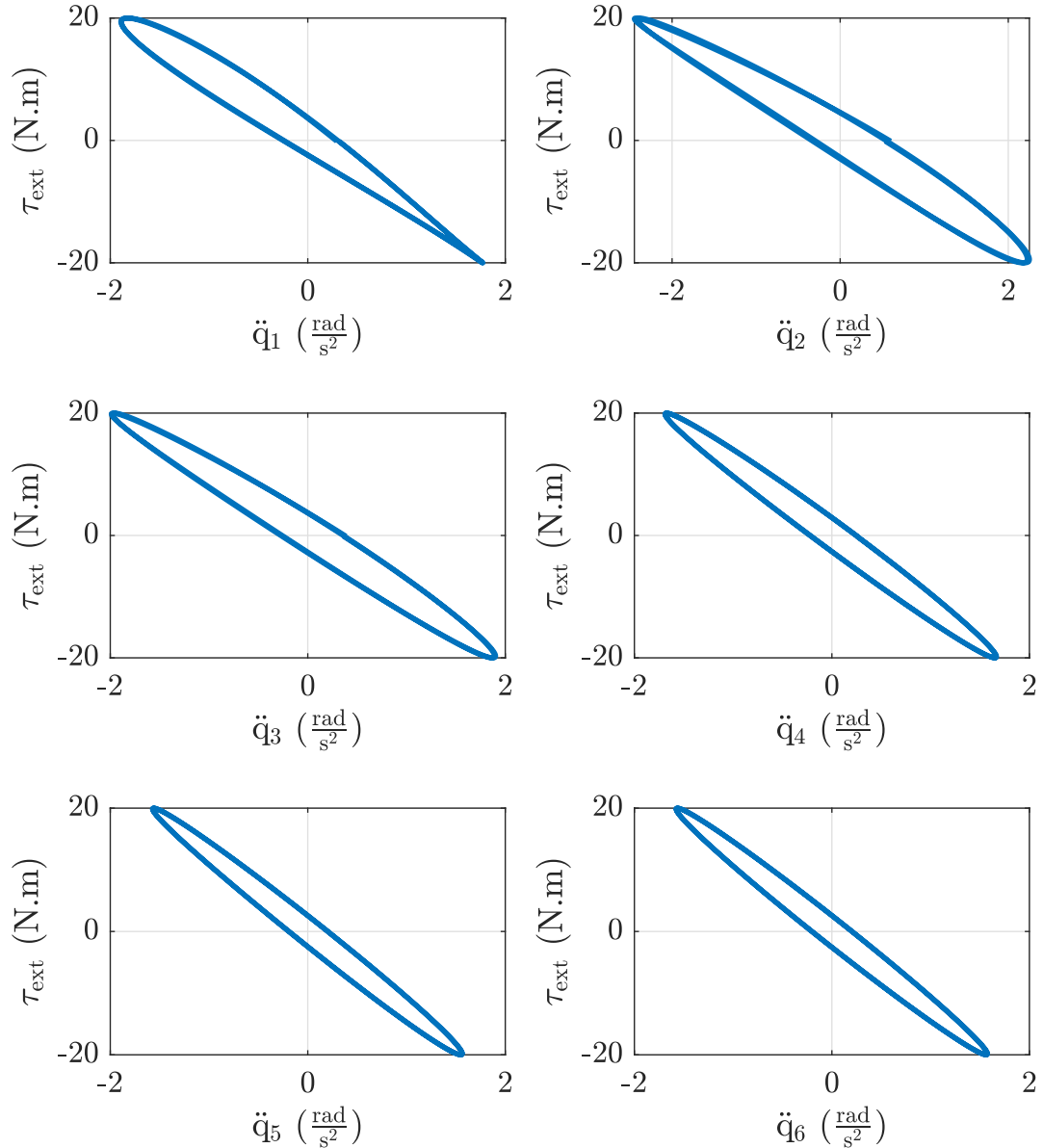


Figure 18: Dynamic relation between external torque (τ_{ext}) and joint accelerations (\ddot{q}) using proportional-derivative impedance control with gravity compensation (4) with $\mathbf{K}_{\text{des}} = 500 \mathbf{I}_{6 \times 6} \frac{\text{N.m}}{\text{rad}}$, $\mathbf{D}_{\text{des}} = 10 \mathbf{I}_{6 \times 6}$ and $\frac{\text{N.m.s}}{\text{rad}}$.

1.3 Inertial dynamic coupling compensation

The objective of this activity is analyze effects inertial couplings on the relation between interaction torques (τ_{ext}) and joint configuration ($\mathbf{q}, \dot{\mathbf{q}}, \ddot{\mathbf{q}}$). For this purpose, a simulation environment is developed that contains the UR5 robot and allows external torques to be applied. The simulation starts with initial joint configuration $\mathbf{q}_0 = [0.0 \ -1.0 \ 1.0 \ 0.5 \ 0.0 \ 0.5]$ rad. Then, external torque $\tau_{\text{ext}} = 20 \sin(2\pi t)$ is applied to each joint. Finally, movements of ur5 robot is controlled with a proportional-derivative impedance control method with inertia and gravity compensation at joint level. Thus, control law can be computed as

$$\boldsymbol{\tau} = \mathbf{M}(\mathbf{K}_{\text{des}}\mathbf{e} + \mathbf{D}_{\text{des}}\dot{\mathbf{e}}) + \mathbf{b}, \quad (5)$$

where $\mathbf{e} = \mathbf{q}_{\text{des}} - \mathbf{q}$ is joint position error, \mathbf{M} is inertia matrix, $\mathbf{b} = \mathbf{C}(\mathbf{q}, \dot{\mathbf{q}}) + \mathbf{g}(\mathbf{q})$ is nonlinear effects vector, and $\mathbf{D}_{\text{des}}, \mathbf{K}_{\text{des}}$ are desired stiffness and damping matrix, respectively.

Figure 19-21 show relation between external torque (τ_{ext}) and joint configuration ($\mathbf{q}, \dot{\mathbf{q}}, \ddot{\mathbf{q}}$) using control law (5) with $\mathbf{K}_{\text{des}} = 500\mathbf{I}_{6 \times 6} \frac{\text{N.m}}{\text{rad}}$, $\mathbf{D}_{\text{des}} = 10\mathbf{I}_{6 \times 6}$ and $\frac{\text{N.m.s}}{\text{rad}}$. In this figures, impedance profiles (τ_{ext} vs $\mathbf{q}, \dot{\mathbf{q}}, \ddot{\mathbf{q}}$) are the same for all joints. Thus, maximum joint position displacement ($\Delta q = 0.04$ rad) and maximum/minimum velocity ($\dot{q} = \pm 2 \frac{\text{rad}}{\text{s}}$) are the same for all joints when robot interact with external torques.

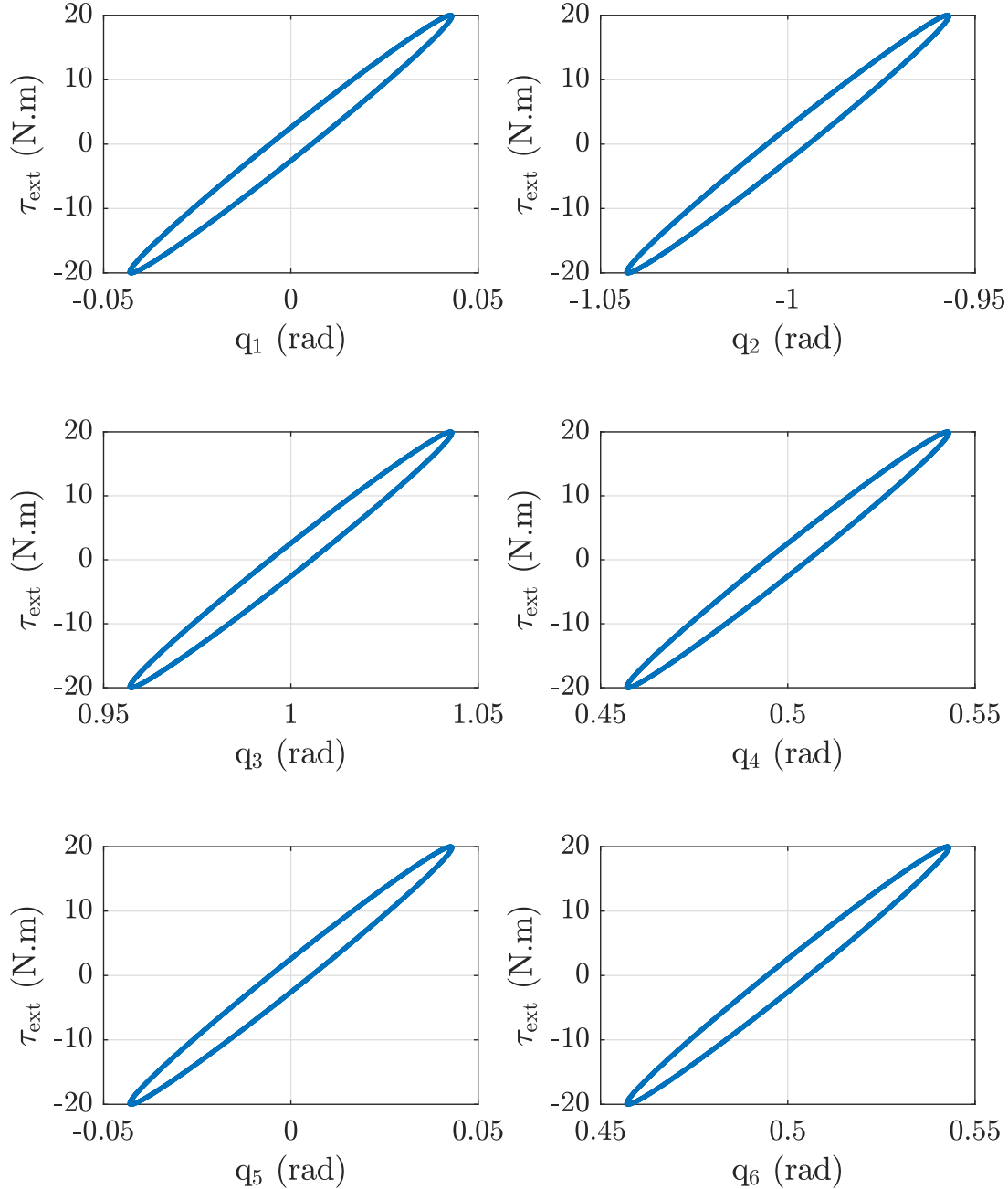


Figure 19: Dynamic relation between external torque (τ_{ext}) and joint positions (q) using proportional-derivative impedance control with inertia and gravity compensation (5) with $\mathbf{K}_{\text{des}} = 500 \mathbf{I}_{6 \times 6} \frac{\text{N.m}}{\text{rad}}$, $\mathbf{D}_{\text{des}} = 10 \mathbf{I}_{6 \times 6}$ and $\frac{\text{N.m.s}}{\text{rad}}$.

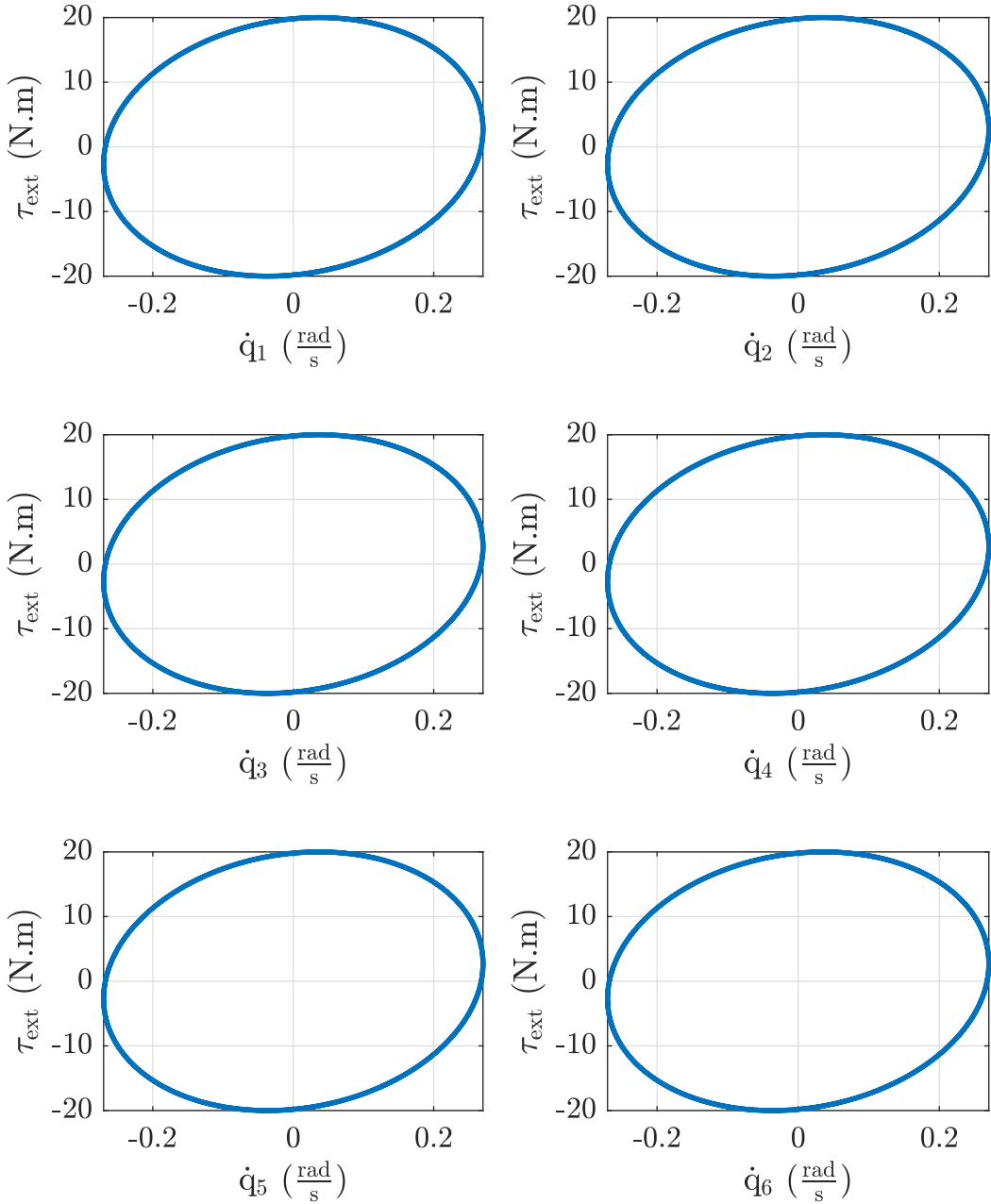


Figure 20: Dynamic relation between external torque (τ_{ext}) and joint velocities (\dot{q}) using proportional-derivative impedance control with inertia and gravity compensation (5) with $\mathbf{K}_{\text{des}} = 500 \mathbf{I}_{6 \times 6} \frac{\text{N.m}}{\text{rad}}$, $\mathbf{D}_{\text{des}} = 10 \mathbf{I}_{6 \times 6}$ and $\frac{\text{N.m.s}}{\text{rad}}$.

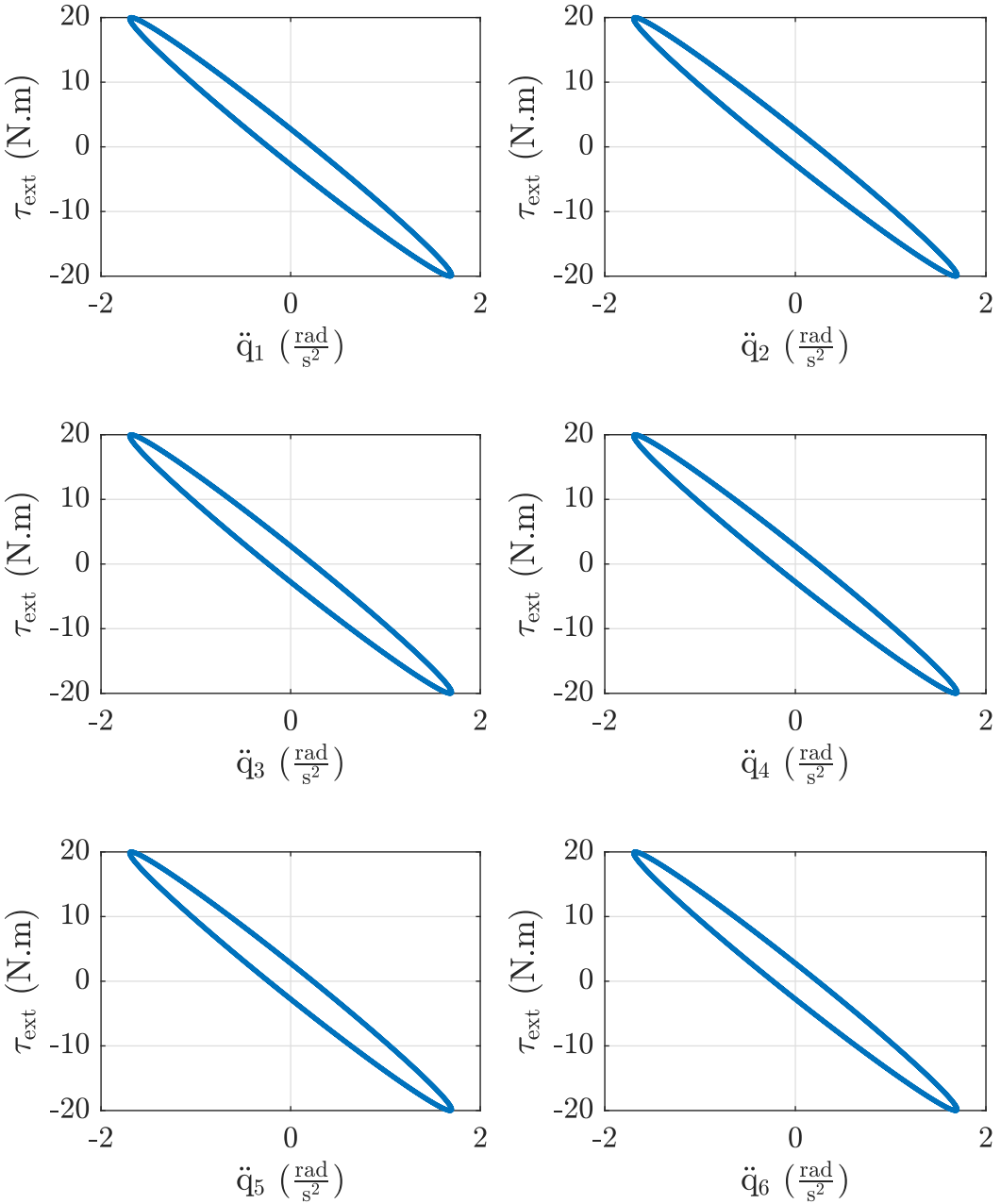


Figure 21: Dynamic relation between external torque (τ_{ext}) and joint accelerations (\ddot{q}_i) using proportional-derivative impedance control with inertia and gravity compensation (5) with $\mathbf{K}_{\text{des}} = 500 \mathbf{I}_{6 \times 6} \frac{\text{N.m}}{\text{rad}}$, $\mathbf{D}_{\text{des}} = 10 \mathbf{I}_{6 \times 6}$ and $\frac{\text{N.m.s}}{\text{rad}}$.

1.4 Inertia control

The objective of this activity is analyze the effects of impedance parameters (\mathbf{M}_{des}) and joint configuration ($\mathbf{q}, \dot{\mathbf{q}}, \ddot{\mathbf{q}}$). For this purpose, a simulation environment is developed that contains the UR5 robot and allows external torques to be applied. The simulation starts with joint configuration $\mathbf{q}_0 = [0.0 \ -1.0 \ 1.0 \ 0.5 \ 0.0 \ 0.5]$ rad. Then, external torque $\tau_{\text{ext}} = 20 \sin(2\pi t)$ N.m is applied to each joint. Finally, movements of ur5 robot is controlled with a mass-proportional-derivative impedance control method with inertia and gravity compensation at joint level. Thus, control law can be computed as

$$\boldsymbol{\tau} = \mathbf{M} (\mathbf{M}_{\text{des}}^{-1} (\mathbf{K}_{\text{des}} \mathbf{e} + \mathbf{D}_{\text{des}} \dot{\mathbf{e}})) + \mathbf{b}, \quad (6)$$

where $\mathbf{e} = \mathbf{q}_{\text{des}} - \mathbf{q}$ is joint position error, \mathbf{M} is inertia matrix, $\mathbf{b} = \mathbf{C}(\mathbf{q}, \dot{\mathbf{q}}) + \mathbf{g}(\mathbf{q})$ is nonlinear effects vector, and $\mathbf{M}_{\text{des}}, \mathbf{D}_{\text{des}}, \mathbf{K}_{\text{des}}$ are desired inertia, stiffness and damping matrix, respectively.

Figure 22-24 show relation between external torque ($\boldsymbol{\tau}_{\text{ext}}$) and joint configuration ($\mathbf{q}, \dot{\mathbf{q}}, \ddot{\mathbf{q}}$) using control law (6) with $\mathbf{M}_{\text{des}} = 0.1 \mathbf{I}_{6 \times 6}$, $\mathbf{K}_{\text{des}} = 500 \mathbf{I}_{6 \times 6}$ and $\mathbf{D}_{\text{des}} = 10 \mathbf{I}_{6 \times 6}$. In this figures, impedance profiles ($\boldsymbol{\tau}_{\text{ext}}$ vs $\mathbf{q}, \dot{\mathbf{q}}, \ddot{\mathbf{q}}$) are the same for all joints. However, maximum joint position displacement change from $\Delta q = 0.04$ rad to $\Delta q = 0.004$ rad whereas maximum/minimum velocity change from $\dot{q} = \pm 2 \frac{\text{rad}}{\text{s}}$ to $\dot{q} = \pm 0.2 \frac{\text{rad}}{\text{s}}$. This is because $\mathbf{M}_{\text{des}}^{-1}$ increase stiffness and damping by 10.

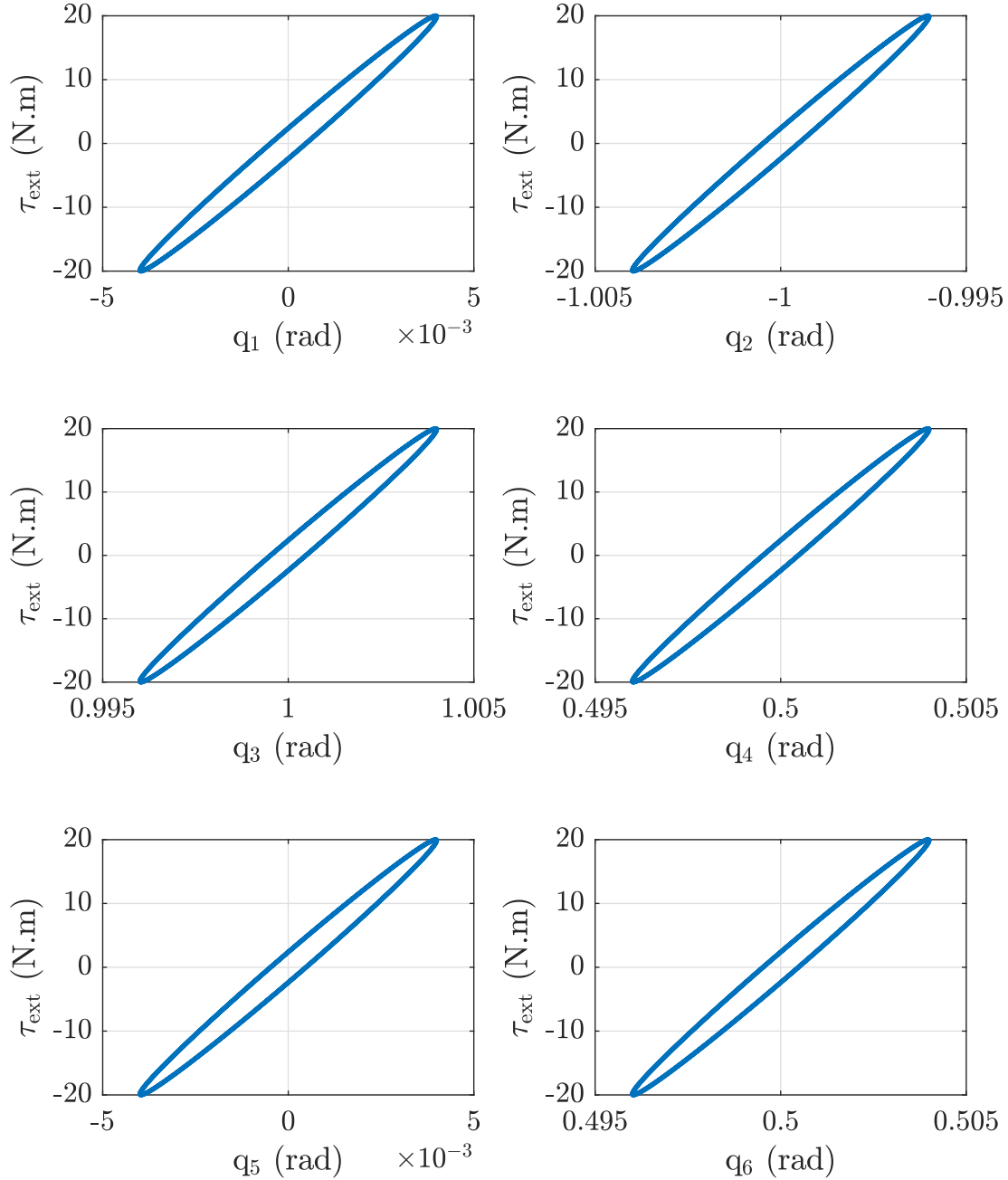


Figure 22: Dynamic relation between external torque (τ_{ext}) and joint positions (q) using mass-proportional-derivative impedance control with inertia and gravity compensation (6) with $\mathbf{M}_{\text{des}} = 0.1 \mathbf{I}_{6 \times 6}$, $\mathbf{K}_{\text{des}} = 500 \mathbf{I}_{6 \times 6} \frac{\text{N.m}}{\text{rad}}$, $\mathbf{D}_{\text{des}} = 10 \mathbf{I}_{6 \times 6}$ and $\frac{\text{N.m.s}}{\text{rad}}$.

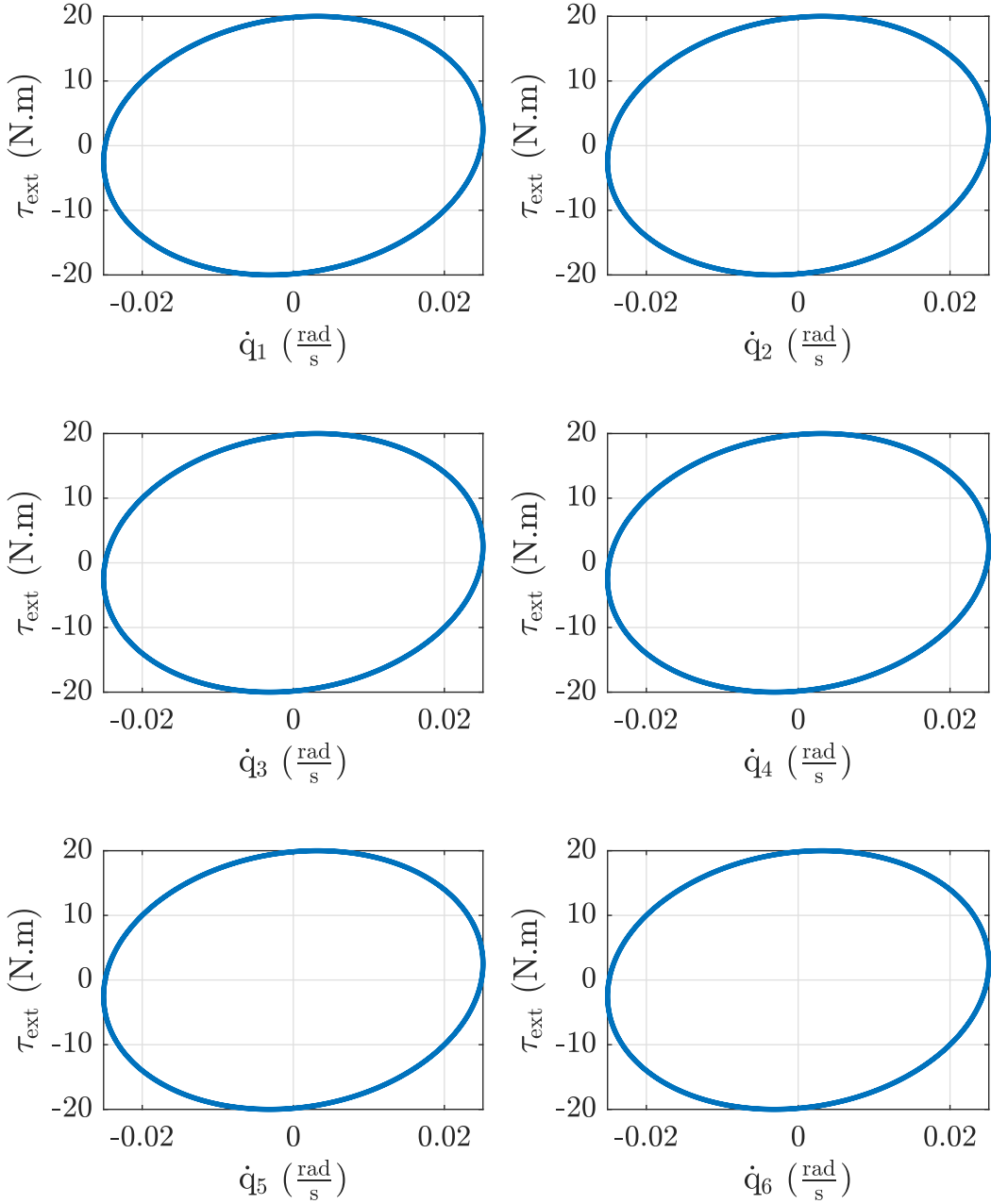


Figure 23: Dynamic relation between external torque (τ_{ext}) and joint velocities (\dot{q}) using mass-proportional-derivative impedance control with inertia and gravity compensation (6) with $M_{\text{des}} = 0.1I_{6 \times 6}$, $K_{\text{des}} = 500I_{6 \times 6} \frac{\text{N.m}}{\text{rad}}$, $D_{\text{des}} = 10I_{6 \times 6}$ and $\frac{\text{N.m.s}}{\text{rad}}$.

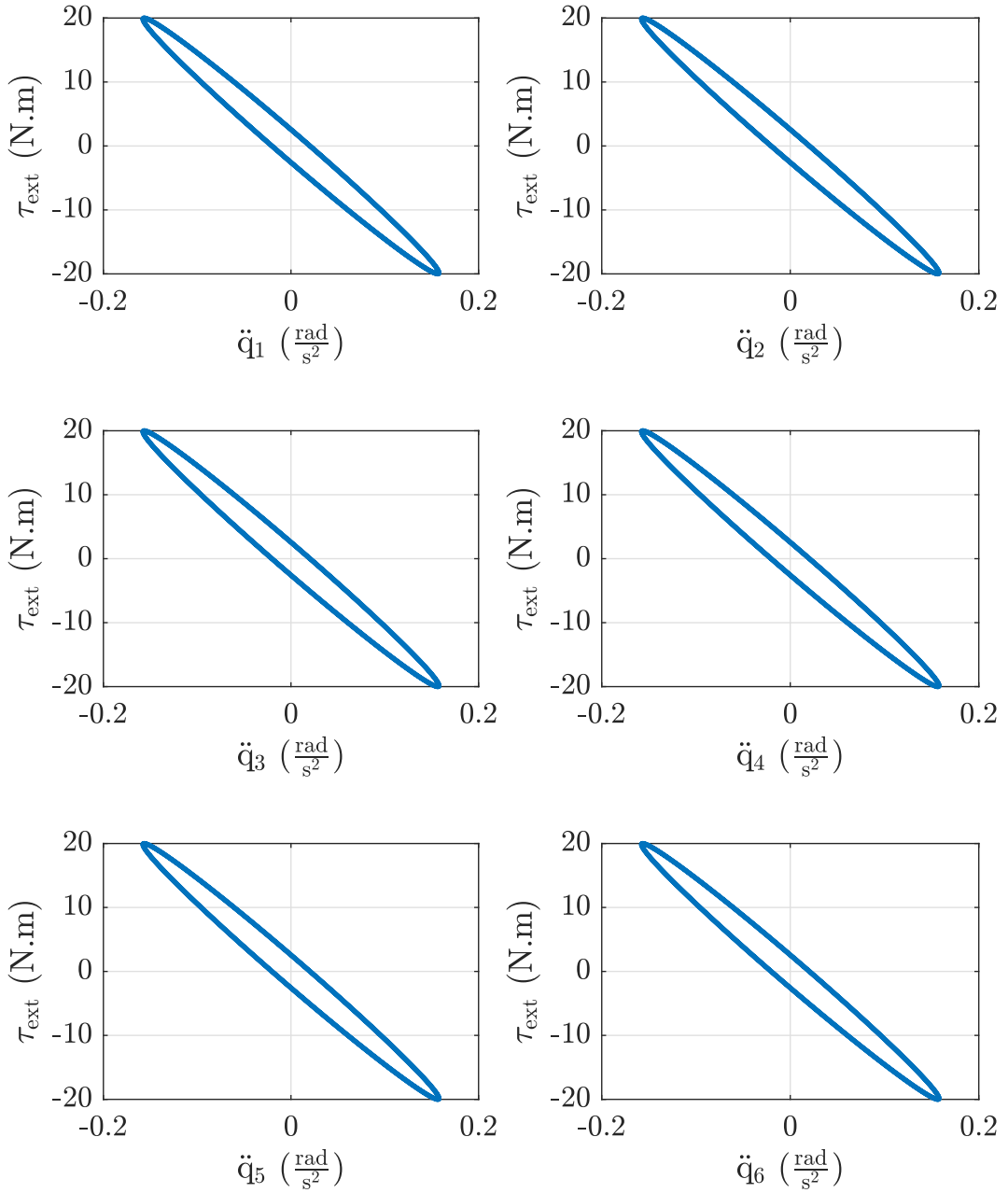


Figure 24: Dynamic relation between external torque (τ_{ext}) and joint accelerations (\ddot{q}) using mass-proportional-derivative impedance control with inertia and gravity compensation (6) with $\mathbf{M}_{\text{des}} = 0.1\mathbf{I}_{6 \times 6}$, $\mathbf{K}_{\text{des}} = 500\mathbf{I}_{6 \times 6} \frac{\text{N.m}}{\text{rad}}$, $\mathbf{D}_{\text{des}} = 10\mathbf{I}_{6 \times 6}$ and $\frac{\text{N.m.s}}{\text{rad}}$.

2 Task space impedance control

2.1 PD impedance control

The objective of this activity is analyze the effects of impedance parameters (\mathbf{K}_{des} , \mathbf{D}_{des}) on the dynamics relation between interaction forces (\mathbf{f}_{ext}) and Cartesian configuration ($\mathbf{x}, \dot{\mathbf{x}}, \ddot{\mathbf{x}}$). For this purpose, a simulation environment is developed that contains the UR5 robot and allows external forces to be applied. The simulation starts with robot end-effector cartesian position $\mathbf{p}_0 = [0.577 \ 0.192 \ 0.364]^T$ m. Then, external force $\mathbf{f}_{\text{ext}} = 50 \sin(2\pi t)$ N is applied to robot end-effector. Finally, motion control is made up of two approaches: cartesian proportional-derivative impedance (PDI) control and projection of the null space. In this sense, cartesian PDI control method focuses on set desired dynamic behavior and the projection of null space maintains the articular position close to \mathbf{q}_0 . Finally, control law can be computed as

$$\boldsymbol{\tau} = \mathbf{J}^T (\mathbf{K}_{\text{des}} \mathbf{e} + \mathbf{D}_{\text{des}} \dot{\mathbf{e}}) + \mathbf{N} (\mathbf{K}_q (\mathbf{q}_0 - \mathbf{q}) - \mathbf{D}_q \dot{\mathbf{q}}), \quad (7)$$

$$\mathbf{N} = (\mathbf{I}_{6 \times 6} - \mathbf{J}^\# \mathbf{J}),$$

where \mathbf{J} is geometric jacobian matrix, $\mathbf{e} = \mathbf{p}_{\text{des}} - \mathbf{p}$ is end-effector position error, and \mathbf{K}_{des} , \mathbf{D}_{des} are desired stiffness and damping, respectively; $\mathbf{J}^\#$ is jacobian damped pseudo-inverse, \mathbf{N} is the null space projection of $\mathbf{J}^\#$, and \mathbf{K}_q , \mathbf{D}_q are the proportional and derivative gains for null space projection.

Figure 25 shows the dynamics relation between external torque ($\boldsymbol{\tau}_{\text{ext}}$) and cartesian configuration ($\mathbf{q}, \dot{\mathbf{q}}, \ddot{\mathbf{q}}$) using control law (7) with $\mathbf{K}_{\text{des}} = 500 \mathbf{I}_{6 \times 6}$ and $\mathbf{D}_{\text{des}} = 50 \mathbf{I}_{6 \times 6}$. In these figures, each cartesian axis (x, y, z) present different dynamic behaviors despite having the same control law. This is because the robot configuration generates different inertial and gravitational effects on each cartesian axis. Thus, impedance profiles can be improved by compensating for inertia and gravitational effects at control law.

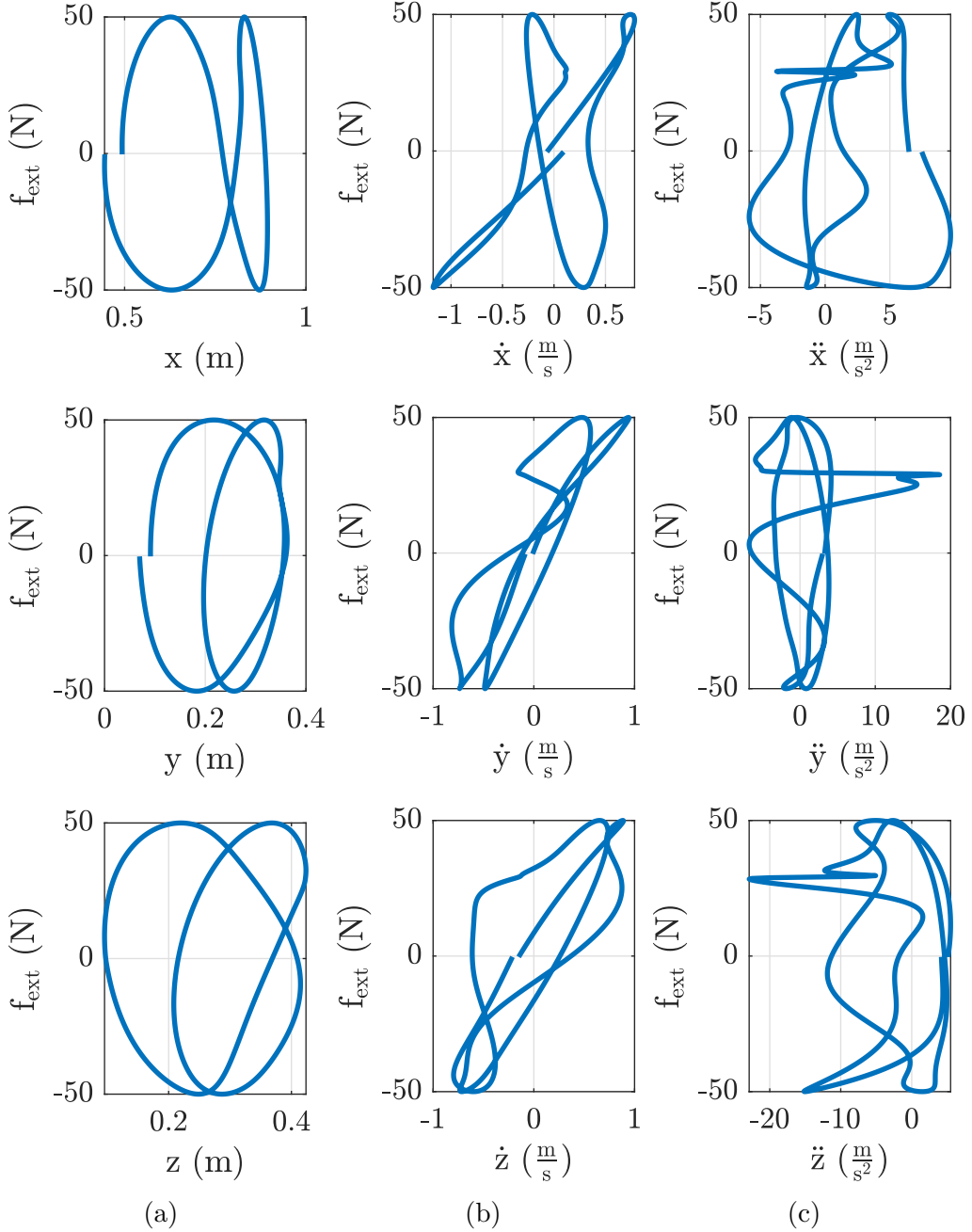


Figure 25: Dynamics relation between external force (\mathbf{f}_{ext}) and cartesian configuration ($\mathbf{x}, \dot{\mathbf{x}}, \ddot{\mathbf{x}}$) using proportional-derivative impedance control (7) with $\mathbf{K}_{\text{des}} = 500\mathbf{I}_{6 \times 6}$ and $\mathbf{D}_{\text{des}} = 50\mathbf{I}_{6 \times 6}$: (a) position, (b) velocity and (c) acceleration.

2.2 Gravity and Coriolis compensation

The objective of this activity is analyze effects of gravity and Coriolis terms on the dynamics relation between interaction forces (\mathbf{f}_{ext}) and Cartesian configuration ($\mathbf{x}, \dot{\mathbf{x}}, \ddot{\mathbf{x}}$). For this purpose, a simulation environment is developed that contains the UR5 robot and allows external forces to be applied. The simulation starts with robot end-effector cartesian position $\mathbf{p}_0 = [0.577 \ 0.192 \ 0.364]$ m. Then, external force $\mathbf{f}_{\text{ext}} = 50 \sin(2\pi t)$ N is applied to robot end-effector. Finally, motion control is made up of two approaches: cartesian proportional-derivative impedance with gravity and Coriolis compensation (PDI+b) control and projection of the null space. In this sense, cartesian PDI+b control method focuses on set desired dynamic behavior and the projection of null space maintains the articular position close to \mathbf{q}_0 . Finally, control law can be computed as

$$\boldsymbol{\tau} = \mathbf{J}^T (\mathbf{K}_{\text{des}} \mathbf{e} + \mathbf{D}_{\text{des}} \dot{\mathbf{e}} + \boldsymbol{\mu}) + \mathbf{N} (\mathbf{K}_{\mathbf{q}} (\mathbf{q}_0 - \mathbf{q}) - \mathbf{D}_{\mathbf{q}} \dot{\mathbf{q}}), \quad (8)$$

$$\begin{aligned} \boldsymbol{\Lambda} &= (\mathbf{J} \mathbf{M}^{-1} \mathbf{J}^T)^{-1}, \\ \boldsymbol{\mu} &= \mathbf{J}^{T\#} - \boldsymbol{\Lambda} \mathbf{J} \dot{\mathbf{q}}, \\ \mathbf{N} &= (\mathbf{I}_{6 \times 6} - \mathbf{J}^\# \mathbf{J}), \end{aligned}$$

where \mathbf{J} is geometric jacobian matrix, $\mathbf{e} = \mathbf{p}_{\text{des}} - \mathbf{p}$ is end-effector position error, and $\mathbf{K}_{\text{des}}, \mathbf{D}_{\text{des}}$ are desired stiffness and damping, respectively; $\mathbf{J}^\#$ is jacobian damped pseudo-inverse, $\boldsymbol{\mu}$ is nonlinear effects vector at Cartesian space, \mathbf{N} is the null space projection of $\mathbf{J}^\#$, and $\mathbf{K}_{\mathbf{q}}, \mathbf{D}_{\mathbf{q}}$ are the proportional and derivative gains for null space projection.

Figure 26 shows the dynamics relation between external torque ($\boldsymbol{\tau}_{\text{ext}}$) and cartesian configuration ($\mathbf{q}, \dot{\mathbf{q}}, \ddot{\mathbf{q}}$) using control law (8) with $\mathbf{K}_{\text{des}} = 500 \mathbf{I}_{6 \times 6}$ and $\mathbf{D}_{\text{des}} = 50 \mathbf{I}_{6 \times 6}$. In these figures, similar dynamic behaviors are observed in Cartesian position graphs due to compensation for gravitational and Coriolis effects. However, in the velocity and acceleration graphs, differences are observed at the beginning and at the end. Finally, impedance profiles can be improved by compensating for inertia at control law.

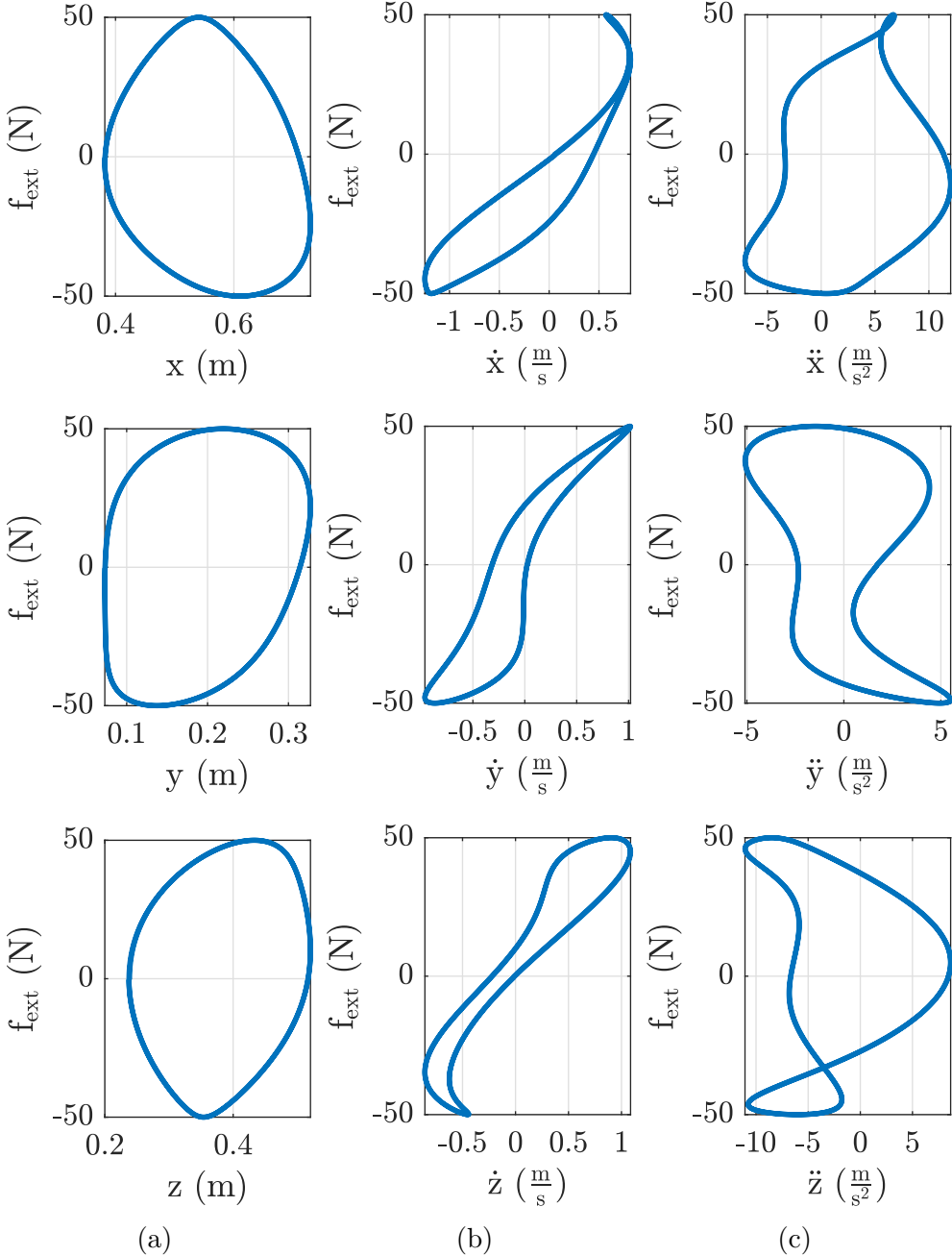


Figure 26: Dynamics relation between external force (f_{ext}) and Cartesian configuration ($\mathbf{x}, \dot{\mathbf{x}}, \ddot{\mathbf{x}}$) using proportional-derivative impedance control (7) with $\mathbf{K}_{\text{des}} = 500\mathbf{I}_{6 \times 6}$ and $\mathbf{D}_{\text{des}} = 50\mathbf{I}_{6 \times 6}$: (a) position, (b) velocity and (c) acceleration.

2.3 Inverse dynamics based impedance control

The objective of this activity is analyze the effects of inertia (Λ) on the dynamic relation between interaction forces (\mathbf{f}_{ext}) and Cartesian configuration ($\mathbf{x}, \dot{\mathbf{x}}, \ddot{\mathbf{x}}$). For this purpose, a simulation environment is developed that contains the UR5 robot and allows external forces to be applied. The simulation starts with robot end-effector Cartesian position $\mathbf{p}_0 = [0.577 \ 0.192 \ 0.364]^T$ m. Then, external force $\mathbf{f}_{\text{ext}} = 50 \sin(2\pi t)$ N is applied to robot end-effector. Finally, motion control is made up of two approaches: Cartesian inverse dynamics based impedance control and projection of the null space. In this sense, Cartesian inverse dynamics based impedance control focuses on set desired dynamic behavior and the projection of null space maintains the articular position close to \mathbf{q}_0 . Finally, control law can be computed as

$$\boldsymbol{\tau} = \mathbf{J}^T (\Lambda(\ddot{\mathbf{p}}_{\text{des}} + \mathbf{K}_{\text{des}}\mathbf{e} + \mathbf{D}_{\text{des}}\dot{\mathbf{e}}) + \boldsymbol{\mu}) + \mathbf{N} (\mathbf{K}_{\mathbf{q}}(\mathbf{q}_0 - \mathbf{q}) - \mathbf{D}_{\mathbf{q}}\dot{\mathbf{q}}), \quad (9)$$

$$\begin{aligned}\Lambda &= (\mathbf{J}\mathbf{M}^{-1}\mathbf{J}^T)^{-1}, \\ \boldsymbol{\mu} &= \mathbf{J}^{T\#} - \Lambda \mathbf{J} \dot{\mathbf{q}}, \\ \mathbf{N} &= (\mathbf{I}_{6 \times 6} - \mathbf{J}^\# \mathbf{J}),\end{aligned}$$

where \mathbf{J} is geometric jacobian matrix, Λ is inertia matrix at Cartesian space, $\mathbf{e} = \mathbf{p}_{\text{des}} - \mathbf{p}$ is end-effector position error, and $\mathbf{K}_{\text{des}}, \mathbf{D}_{\text{des}}$ are desired stiffness and damping, respectively; $\mathbf{J}^\#$ is jacobian damped pseudo-inverse, $\boldsymbol{\mu}$ is nonlinear effects vector at cartesian space, \mathbf{N} is the null space projection of $\mathbf{J}^\#$, and $\mathbf{K}_{\mathbf{q}}, \mathbf{D}_{\mathbf{q}}$ are the proportional and derivative gains for null space projection.

Figure 27 shows the dynamics relation between external force (\mathbf{f}_{ext}) and cartesian configuration ($\mathbf{x}, \dot{\mathbf{x}}, \ddot{\mathbf{x}}$) using control law (9) with $\mathbf{K}_{\text{des}} = 500\mathbf{I}_{6 \times 6}$ and $\mathbf{D}_{\text{des}} = 50\mathbf{I}_{6 \times 6}$. In these figures, similar dynamic behaviors are observed in Cartesian position and velocity graphs due to compensation for inertia, gravitational and Coriolis effects. Finally, differences in Cartesian acceleration graphs could be generated by null space terms.

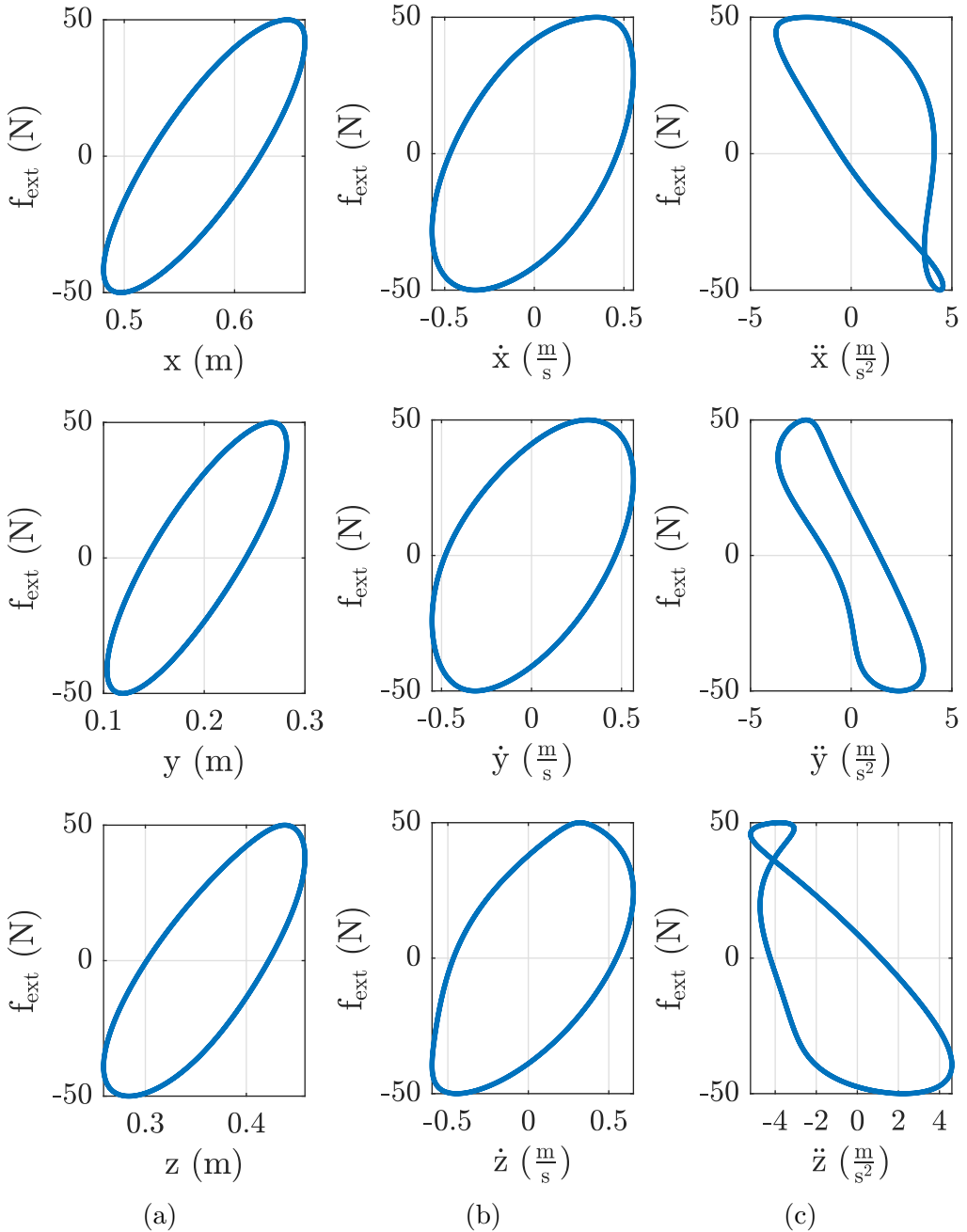


Figure 27: Dynamic relation between external force (\mathbf{f}_{ext}) and Cartesian configuration ($\mathbf{x}, \dot{\mathbf{x}}, \ddot{\mathbf{x}}$) using inverse dynamic based impedance control (9) with $\mathbf{K}_{\text{des}} = 500\mathbf{I}_{6 \times 6}$ and $\mathbf{D}_{\text{des}} = 50\mathbf{I}_{6 \times 6}$: (a) position, (b) velocity and (c) acceleration.